William R. Leo

Techniques for Nuclear and Particle Physics Experiments

A How-to Approach

Second Revised Edition
With 256 Figures, 40 Tables and Numerous Worked Examples

Springer-Verlag
Berlin Heidelberg New York
London Paris Tokyo
Hong Kong Barcelona
Budapest

5. General Characteristics of Detectors

As an introduction to the following chapters on detectors, we will define and describe here some general characteristics common to detectors as a class of devices. For the reader without detector experience, these characteristics will probably take on more significance when examples of specific detectors are treated. He should not hesitate to continue on, therefore, and return at a later time if he has not fully understood the contents of this chapter.

While the history of nuclear and elementary particle physics has seen the development of many different types of detectors, all are based on the same fundamental principle. the transfer of part or all of the radiation energy to the detector mass where it is converted into some other form more accessible to human perception. As we have seen in Chap 2, charged particles transfer their energy to matter through direct collisions with the atomic electrons, thus inducing excitation or ionization of the atoms. Neutral radiation, on the other hand, must first undergo some sort of reaction in the detector producing charged particles, which in turn ionize and excite the detector atoms. The form in which the converted energy appears depends on the detector and its design. The gaseous detectors discussed in the next chapter, for example, are designed to directly collect the ionization electrons to form an electric current signal, while in scintillators, both the excitation and ionization contribute to inducing molecular transitions which result in the emission of light Similarly, in photographic emulsions, the ionization induces chemical reactions which allow a track image to be formed, and so on.

Modern detectors today are essentially electrical in nature, i.e., at some point along the way the information from the detector is transformed into electrical impulses which can be treated by electronic means. This, of course, takes advantage of the great progress that has been made in electronics and computers to provide for faster and more accurate treatment of the information. Indeed, most modern detectors cannot be exploited otherwise. When discussing "*detectors*", therefore, we will also take this to mean the electronics as well. This, of course, is not to say that only electrical detectors are used in modern experiments, and indeed there are many other types which are employed. However, if an electrical detector can be used, it is generally preferred for the reasons already mentioned. Our discussion in the following sections, therefore, will only be concerned with this type.

5.1 Sensitivity

The first consideration for a detector is its sensitivity, i.e., its capability of producing a usable signal for a given type of radiation and energy No detector can be sensitive to all types of radiation at all energies. Instead, they are designed to be sensitive to certain types of radiation in a given energy range. Going outside this region usually results in an unusable signal or greatly decreased efficiency.

Detector sensitivity to a given type of radiation of a given energy depends on several factors:

1) the cross section for ionizing reactions in the detector
2) the detector mass
3) the inherent detector noise
4) the protective material surrounding the sensitive volume of the detector.

The cross-section and detector mass determine the probability that the incident radiation will convert part or all its energy in the detector into the form of ionization. (We assume here that the properties of the detector are such that the ionization created will be efficiently used.) As we saw in Chap. 2, charged particles are highly ionizing, so that most detectors even of low density and small volume will have some ionization produced in their sensitive volume. For neutral particles, this is much less the case, as they must first undergo an interaction which produces charged particles capable of ionizing the detector medium. These interaction cross sections are usually much smaller so that a higher mass density and volume are necessary to ensure a reasonable interaction rate, otherwise the detector becomes essentially transparent to the neutral radiation. The mass required, depends on the type of radiation and the energy range of interest In the case of the neutrino, for example, detector masses on the order of tons are usually necessary!

Even if ionization is produced in the detector, however, a certain minimum amount is necessary in order for the signal to be usable. This lower limit is determined by the noise from the detector and the associated electronics. The noise appears as a fluctuating voltage or current at the detector output and is always present whether there is radiation or not. Obviously, the ionization signal must be larger than the average noise level in order to be usable. For a given radiation type in a given energy range, the total amount of ionization produced is determined by the sensitive volume.

A second limiting factor is the material covering the entrance window to the sensitive volume of the detector Because of absorption, only radiation with sufficient energy to penetrate this layer can be detected. The thickness of this material thus sets a lower limit on the energy which can be detected.

5.2 Detector Response

In addition to detecting the presence of radiation, most detectors are also capable of providing some information on the energy of the radiation. This follows since the amount of ionization produced by radiation in a detector is proportional to the energy it loses in the sensitive volume. If the detector is sufficiently large such that the radiation is completely absorbed, then this ionization gives a measure of the energy of the radiation. Depending on the design of the detector, this information may or may not be preserved as the signal is processed, however.

In general, the output signal of electrical detectors is in the form of a current pulse[1]. The amount of ionization is then reflected in the electrical charge contained in this

[1] Detectors may also be operated in a continuous mode in which the signal is a continuous current or voltage varying in time with the intensity of the radiation This can be performed by electrically integrating the number of pules over a certain period of time

signal, i.e., the integral of the pulse with respect to time Assuming that the shape of the pulse does not change from one event to the other, however, this integral is directly proportional to the amplitude or *pulse height* of the signal, so that this characteristic may be used instead. The relation between the radiation energy and the total charge or pulse height of the output signal is referred to as the *response* of the detector.

Ideally, of course, one would like this relation to be linear although it is not absolutely necessary. It does, however, simplify matters greatly when transforming the measured pulse height to energy. For many detectors, the response is linear or approximately so over a certain range of energies. In general, however, the response is a function of the particle type and energy, and it does not automatically follow that a detector with a linear response for one type of radiation will be linear for another. A good example is organic scintillator. As will be seen later, the response is linear for electrons down to a very low energies but is nonlinear for heavier particles such as the proton, deuteron, etc. This is due to the different reaction mechanisms which are triggered in the medium by the different particles.

5.3 Energy Resolution. The Fano Factor

For detectors which are designed to measure the energy of the incident radiation, the most important factor is the energy resolution. This is the extent to which the detector can distinguish two close lying energies. In general, the resolution can be measured by sending a monoenergetic beam of radiation into the detector and observing the resulting spectrum. Ideally, of course, one would like to see a sharp delta-function peak. In reality, this is never the case and one observes a peak structure with a finite width, usually Gaussian in shape. This width arises because of fluctuations in the number of ionizations and excitations produced.

The resolution is usually given in terms of the *full width at half maximum* of the peak (FWHM). Energies which are closer than this interval are usually considered unresolvable. This is illustrated in Fig. 5.1. If we denote this width as ΔE, then the relative resolution at the energy E is

$$\text{Resolution} = \Delta E/E\,. \tag{5.1}$$

Equation (5.1) is usually expressed in percent. A NaI detector has about a 8% or 9% resolution for γ-rays of about 1 MeV, for example, while germanium detectors have resolutions on the order of 0.1%!

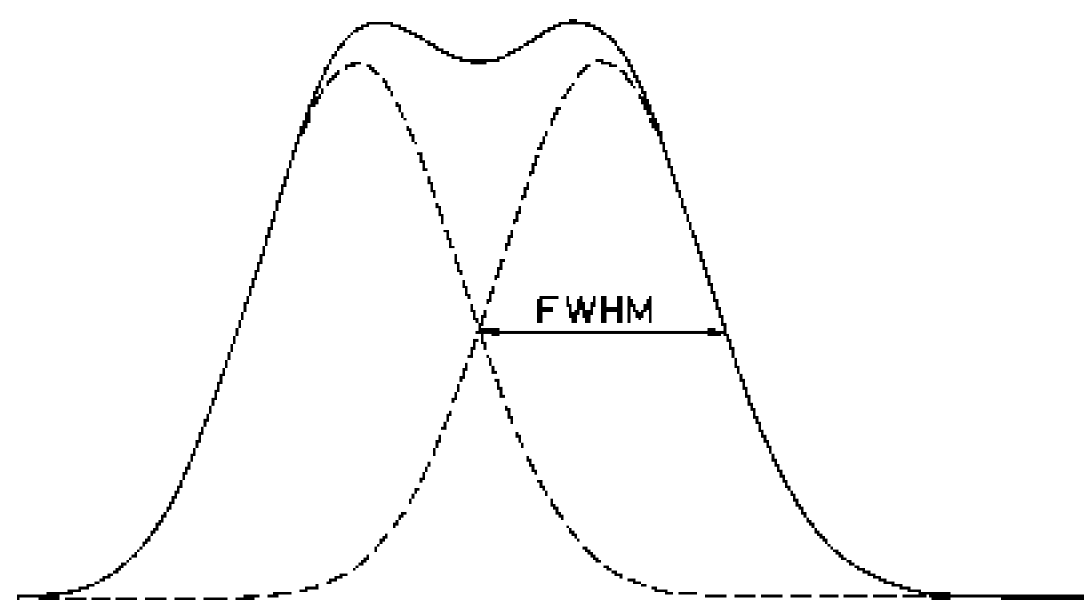

Fig. 5.1. Definition of energy resolution Two peaks are generally considered to be resolved if they are separated by a distance greater than their full widths at half maximum (FWHM) The *solid line* shows the sum of two identical Gaussian peaks separated by just this amount

In general, the resolution is a function of the energy deposited in the detector, with the ratio (5.1) improving with higher energy. This is due to the Poisson or Poisson-like statistics of ionization and excitation. Indeed, it is found that the average energy required to produce an ionization is a fixed number, w, dependent only on the material. For a deposited energy E, therefore, one would expect on the average, $J = E/w$ ionizations. Thus as energy increases, the number of the ionization events also increases resulting in smaller relative fluctuations.

To calculate the fluctuations it is necessary to consider two cases. For a detector in which the radiation energy is not totally absorbed, for example, a thin transmission detector which just measures the dE/dx loss of a passing particle, the number of signal-producing reactions is given by a Poisson distribution. The variance is then given by

$$\sigma^2 = J\,, \tag{5.2}$$

where J is the mean number of events produced. The energy dependence of the resolution can then be seen to be

$$R = 2.35\,\frac{\sqrt{J}}{J} = 2.35\,\sqrt{\frac{w}{E}}\,, \tag{5.3}$$

where the factor 2.35 relates the standard deviation of a Gaussian to its FWHM. Thus the resolution varies inversely as the square root of the energy.

If the full energy of the radiation is absorbed as is the case for detectors used in spectroscopy experiments, the naive assumption of Poisson statistics is incorrect. And indeed, it is observed that the resolution of many such detectors is actually smaller than that calculated from Poisson statistics. The difference here is that the total energy deposited is a fixed, constant value, while in the previous case, the energy deposited can fluctuate. The total number of ionizations which can occur and the energy lost in each ionization are thus constrained by this value. Statistically, this means that the ionization events are not all independent so that Poisson statistics is not applicable. *Fano* [5.1] was the first to calculate the variance under this condition and found

$$\sigma^2 = FJ\,, \tag{5.4}$$

where J is the mean ionization produced and F is a number known as the Fano factor.

The factor F is a function of all the various fundamental processes which can lead to an energy transfer in the detector. This includes all reactions which do not lead to ionization as well, for example, phonon excitations, etc. It is thus an intrinsic constant of the detecting medium. Theoretically, F is very difficult to calculate accurately as it requires a detailed knowledge of all the reactions which can take place in the detector. From (5.4), the resolution is then given by

$$R = 2.35\,\frac{\sqrt{FJ}}{J} = 2.35\,\sqrt{\frac{Fw}{E}}\,. \tag{5.5}$$

If $F = 1$, the variance is the same as that for a Poisson distribution and (5.5) reduces to (5.3). This seems to be the case for scintillators, however, for many detectors such as semiconductors or gases, $F < 1$. This, of course, greatly increases the resolution of these types of detectors.

In addition to the fluctuations in ionization, a number of external factors can affect the overall resolution of a detector. This includes effects from the associated electronics such as noise, drifts, etc. Assuming all these sources are independent and distributed as Gaussians, the total resolution E is then given by (4.64), i.e.,

$$(\Delta E)^2 = (\Delta E_{\mathrm{det}})^2 + (\Delta E_{\mathrm{elect}})^2 + \dots \, . \tag{5.6}$$

5.4 The Response Function

For the measurement of energy spectra, an important factor which must be considered is the *response function* of the detector for the type of radiation being detected. This is the spectrum of pulse heights observed from the detector when it is bombarded by a monoenergetic beam of the given radiation. Up to now, we have assumed that this response spectrum is a Gaussian peak. If we ignore the finite width for a moment, this essentially corresponds to a Dirac delta function, i.e., for a fixed incident energy the output signal has a single, fixed amplitude. Then, if the response is linear, the spectrum of pulse heights measured from the detector corresponds directly to the energy spectrum of the incident radiation. This is the ideal case. Unfortunately, a Gaussian peak response is not always realized particularly in the case of neutral radiation.

The response function of a detector at a given energy is determined by the different interactions which the radiation can undergo in the detector and its design and geometry. To take an example, consider monoenergetic charged particles, say electrons, incident on a detector thick enough to stop the particles. Assuming all the electrons lose their energy by atomic collisions, it is clear that the spectrum of pulse heights will be a Gaussian peak. In reality, however, some of the electrons will scatter out of the detector before fully depositing their energy. This produces a low energy tail. Similarly some electrons will emit bremsstrahlung photons which may escape from the detector. This again gives rise to events at a lower energy than the peak. The response function thus consists of a Gaussian peak with a low energy tail determined by the amount of scattering and bremsstrahlung energy loss. If the tail is small, however, this can still be a reasonable approximation to the ideal Gaussian response depending on the precision desired. Moreover, the response function can be improved by changing the design and geometry of the detector. A material of lower atomic number Z can be chosen, for example, to minimize backscattering and bremsstrahlung. Similarly if the detector is made to surround the source, backscattering electrons will be captured thus decreasing the escape of these particles, etc.

To see how the response function can change with radiation type, consider the same detector with gamma rays instead. As we have already mentioned, gamma rays must first convert into charged particles in order to be detected. The principal mechanisms for this are the photoelectric effect, Compton scattering and pair production. In the photoelectric effect, the gamma ray energy is transferred to the photoelectron which is then stopped in the detector. Since the energy of all the photoelectrons is the same, this results in a sharp peak in the pulse height spectrum, which is the desired Gaussian response. However, some gamma rays will also suffer Compton scatterings. As given by (2.113), the Compton electrons are distributed continuously in energy so that a distribution, similar to Fig. 2.24, also appears in the response function. This, of course,

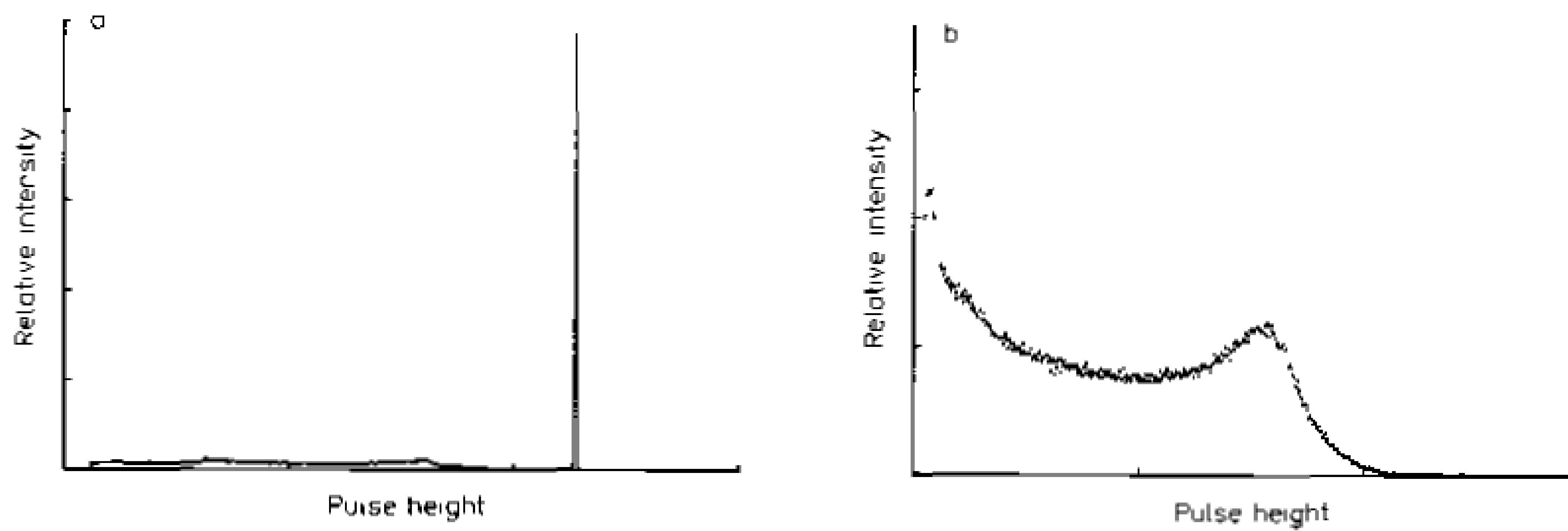

Fig. 5.2a, b. The response functions of two different detectors for 661 keV gamma rays (**a**) shows the response of a germanium detector which has a large photoelectric cross section relative to the Compton scattering cross section at this energy A large photopeak with a relatively small continuous Compton distribution is thus observed (**b**) is the response of an organic scintillator detector. Since this material has a low atomic number Z, Compton scattering is predominant and only this distribution is seen in the response function

immediately destroys the ideal delta-function response. In a similar manner, those events interacting via the pair production mechanism will also contribute a structure to the function. One such total response function is sketched in Fig. 5.2. The observed pulse height spectrum, therefore, simply reflects the different interactions which occur in the detector volume. Since the relative intensity of each structure in the spectrum is determined by the relative cross sections for each interaction mechanism, the response function will also be different at different energies and for different detector media.

If the detector is now used to measure a spectrum of gamma rays, the observed pulse height distribution will be a convolution of the gamma ray spectrum and the detector response, i.e.,

$$PH(E) = \int S(E')R(E, E')\,dE' , \tag{5.7}$$

where $R(E, E')$ is the response function at the incident energy E' and $S(E')$ is the spectrum of gamma ray energies. To determine the gamma ray spectrum $S(E')$, from the measured pulse height distribution then requires knowing $R(E, E')$ in order to invert (5.7). Here, of course, we see the utility of having $R(E, E') = \delta(E'-E)$!

5.5 Response Time

A very important characteristic of a detector is its response time. This is the time which the detector takes to form the signal after the arrival of the radiation. This is crucial to the timing properties of the detector. For good timing, it is necessary for the signal to be quickly formed into a sharp pulse with a rising flank as close to vertical as possible In this way a more precise moment in time is *marked* by the signal.

The duration of the signal is also of importance. During this period, a second event cannot be accepted either because the detector is insensitive or because the second signal will *pile up* on the first. This contributes to the *dead* time of the detector and limits the count rate at which it can be operated. The effect of dead time is discussed in Sect. 5.7.

5.6 Detector Efficiency

Two types of efficiency are generally referred to when discussing radiation detection: *absolute* efficiency and *intrinsic* detection efficiency. The absolute or total efficiency of a detector is defined as that fraction of events emitted by the source which is actually registered by the detector, i.e.,

$$\mathscr{E}_{tot} = \frac{\text{events registered}}{\text{events emitted by source}} . \tag{5.8}$$

This is a function of the detector geometry and the probability of an interaction in the detector. As an example, consider a cylindrical detector with a point source at a distance d on the detector axis as shown in Fig. 5.3. If the source emits isotropically, then, the probability of the particle being emitted at an angle θ is

$$P(\theta)\,d\Omega = d\Omega/4\pi . \tag{5.9}$$

The probability that a particle hitting the detector will have an interaction in the detector is given by (2.7). Combining the two then yields

$$d\mathscr{E}_{tot} = \left[1 - \exp\left(\frac{-x}{\lambda}\right)\right]\frac{d\Omega}{4\pi} , \tag{5.10}$$

where x is the path length in the detector and λ is the mean free path for an interaction The total efficiency is then found by integrating (5.10) over the volume of the detector.

In many cases, however, the value of x does not vary too much over the detector or the value of λ is so small that the exponential can be considered as zero. The absolute efficiency can then be factored into two parts: the *intrinsic* efficiency, $\mathscr{E}_{int}$, and the *geometrical* efficiency or *acceptance*, $\mathscr{E}_{geom}$. The total or absolute efficiency of the detector is then given by the product

$$\mathscr{E}_{tot} \simeq \mathscr{E}_{int}\,\mathscr{E}_{geom} . \tag{5.11}$$

The intrinsic efficiency is that fraction of events actually hitting the detector which is registered, i.e.,

$$\mathscr{E}_{int} = \frac{\text{events registered}}{\text{events impinging on detector}} . \tag{5.12}$$

This probability depends on the interaction cross sections of the incident radiation on the detector medium. The intrinsic efficiency is thus a function of the type of radiation,

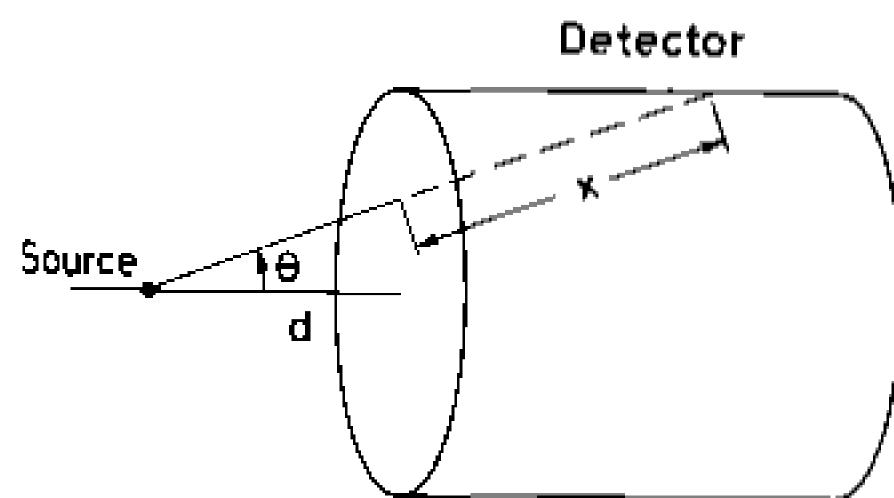

Fig. 5.3. Calculating the detection efficiency of a cylindrical detector for a point source

its energy and the detector material. For charged particles, the intrinsic efficiency is generally good for most detectors, since it is rare for a charged particle *not* to produce some sort of ionization. For heavier particles, though, quenching effects may be present in some materials which drain the ionization produced. The problem of efficiency is generally more important for neutral particles as they must first interact to create secondary charged particles. These interactions are much rarer in general, so that capturing a good fraction of the incident neutral radiation is not always assured. The dimensions of the detector become important as sufficient mass must be present in order to provide a good probability of interaction

The geometric efficiency, in contrast, is that fraction of the source radiation which is geometrically intercepted by the detector. This, of course, depends entirely on the geometrical configuration of the detector and source. The angular distribution of the incident radiation must also be taken into account. For the cylindrical detector in Fig. 5.3, $\mathscr{E}_{geom}$ is simply the average solid angle fraction. For multidetector systems, where coincidence requirements are imposed, however, the calculations can be somewhat complicated and recourse to numerical simulation with Monte Carlo methods must be made

5.7 Dead Time

Related to the efficiency is the *dead time* of the detector. This is the finite time required by the detector to process an event which is usually related to the duration of the pulse signal Depending on the type, a detector may or may not remain sensitive to other events during this period. If the detector is insensitive, any further events arriving during this period are lost. If the detector retains its sensitivity, then, these events may *pile-up* on the first resulting in a distortion of the signal and subsequent loss of information from both events. These losses affect the observed count rates and distort the time distribution between the arrival of events. In particular, events from a random source will no longer have the Poissonian time distribution given by (4.60). To avoid large dead time effects, the counting rate of the detector must be kept sufficiently low such that the probability of a second event occurring during a dead time period is small. The remaining effect can then be corrected.

When calculating the effects of dead time, the entire detection system must be taken into account. Each element of a detector system has it own dead time and, indeed, it is often the electronics which account for the larger part of the effect. Moreover, when several elements have comparable dead times, combining the effects is also a difficult task and a general method does not exist for solving such problems.

As an illustration let us analyze the effect on count rate due to the dead time of a simple element in the system Suppose the element has a dead time τ and that τ is constant for all events. Two fundamental cases are usually distinguished: *extendable* or *non-extendable* dead times. These are also referred to as the *paralyzable* or *non-paralyzable* models In the extendable case, the arrival of a second event during a dead time period extends this period by adding on its dead time τ starting from the moment of its arrival. This is illustrated in Fig. 5.4. This occurs in elements which remain sensitive during the dead time. In principle if the event rate is sufficiently high, events can arrive such that their respective dead time periods all overlap. This produces a prolonged period during which no event is accepted. The element is thus *paralyzed*. The non-

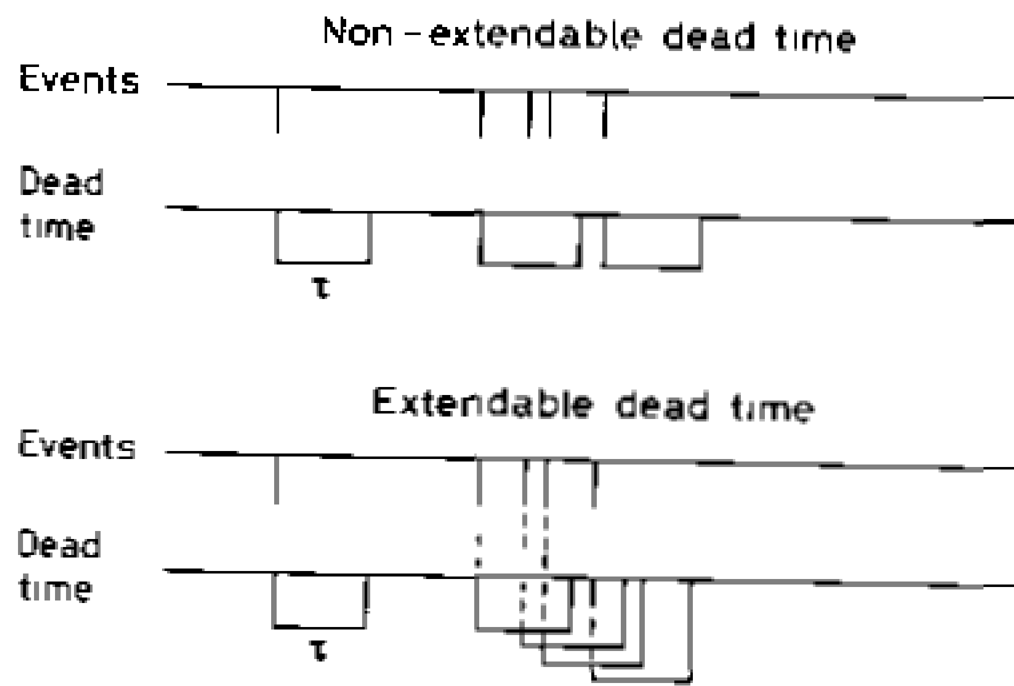

Fig. 5.4. Extendable (paralyzable) and non extendable (non-paralyzable) dead time models

extendable case, in contrast, corresponds to a element which is insensitive during the dead time period. The arrival of a second event during this period simply goes unnoticed and after a time τ the element becomes active again.

Let us consider the non-extendable case first. Suppose m is the true count rate and the detector registers k counts in a time T. Since each detected count n engenders a dead time τ, a total dead time $k\tau$ is accumulated during the counting period T. During this dead period, a total of $mk\tau$ counts is lost. The true number of counts is therefore

$$mT = k + mk\tau . \tag{5.13}$$

Solving for m in terms of k, we find

$$m = \frac{k/T}{1-(k/T)\tau} . \tag{5.14}$$

Thus (5.14) provides us with a formula for finding the true rate m from the observed rate k/T.

The extendable case is somewhat more difficult. Here, one realizes that only those counts which arrive at time intervals greater than τ are recorded. As given by (4.60), the distribution of time intervals between events decaying at a rate m, is

$$P(t) = m \exp(-mt) . \tag{5.15}$$

The probability that $t > \tau$ is then

$$P(t>\tau) = m \int_{\tau}^{\infty} \exp(-mt)\,dt = \exp(-m\tau) . \tag{5.16}$$

The number of counts observed in a time T, therefore, is just that fraction of the mT true events whose arrival times satisfy this condition,

$$k = mT \exp(-m\tau) . \tag{5.17}$$

To find the true value, m, (5.17) must be solved numerically. Figure 5.5 shows the behavior of (5.17). Note that the function first increases, goes through a maximum at $m = 1/\tau$ and then decreases once again. This means that for a given observed rate, k/T, there are two corresponding solutions for m. Care should be taken, therefore, to distinguish between the two.

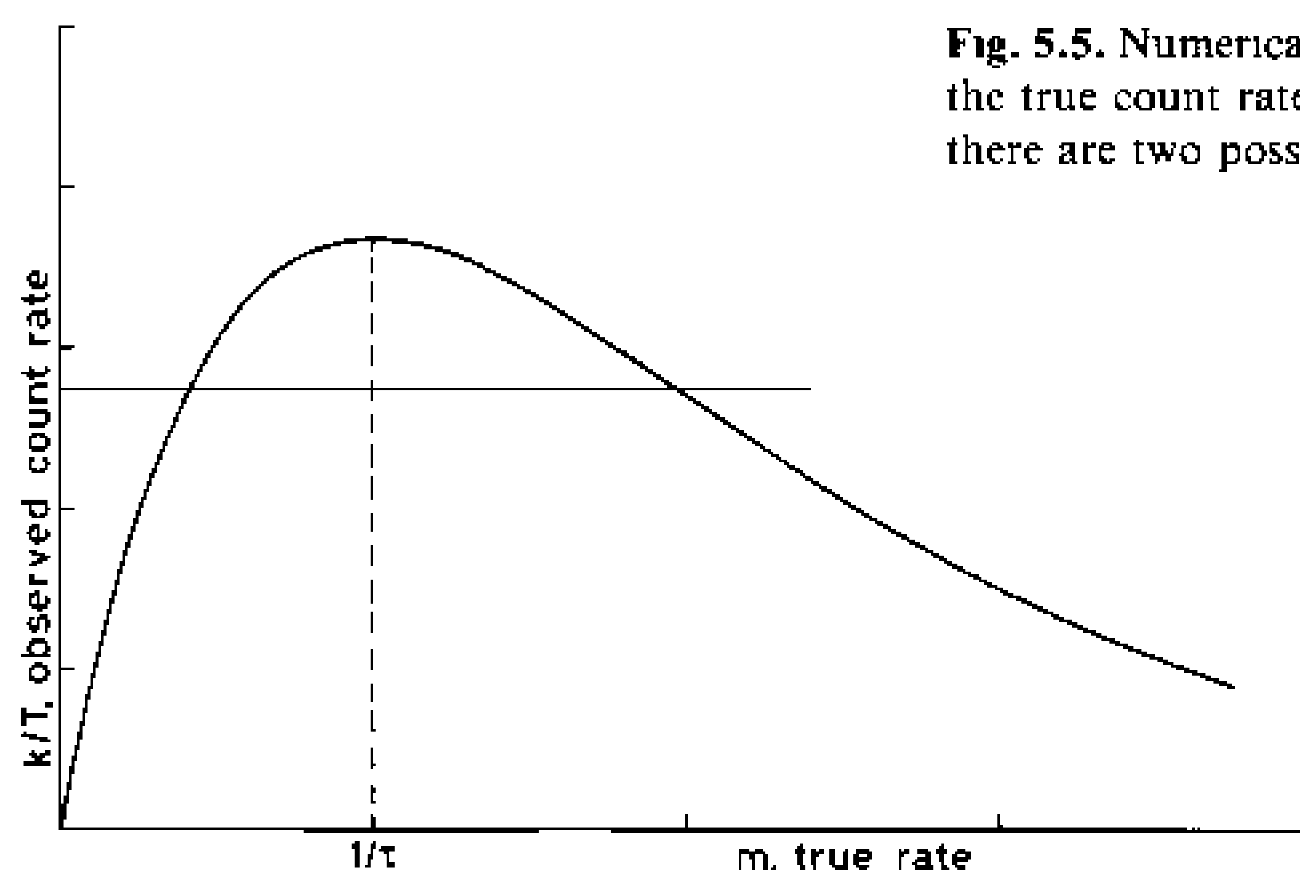

Fig. 5.5. Numerical solution of equation (5 17) to determine the true count rate in the extended dead time model Note there are two possible solutions

The above results are generally adequate for most practical problems, however, they are only first order approximations. More rigorous treatments are given by *Foglio Parra* and *Mandelli Bettoni* [5.2] and a general discussion of dead time problems by *Muller* [5.3]. The case of a variable dead time is also treated by *Libert* [5.4].

Given the above results, the problem which often arises is to determine which class, extendable or non-extendable, is applicable. Indeed, many detectors systems are combinations of both, having some elements which are extendable and others which are not. And some may not be in either class. Moreover the dead time of the elements could be variable depending on the count rate, the pulse shapes, etc. A solution often used is to deliberately add in a blocking circuit element with a dead time larger than all other elements into the system such that the detector system can be treated by one of the fundamental models. This, of course, slows down the system but removes the uncertainty in the dead-time model. This should be done quite early in the system, however, in order to avoid pile-up problems later. See for example the *Inhibit* in Chap. 16.

5.7.1 Measuring Dead Time

The classical method of measuring dead time is the so-called *two-source* technique. In this procedure, the count rates of two different sources are measured separately and together. To illustrate the principle of the method, let us suppose n_1 and n_2 are the true count rates of the two sources and R_1, R_2 and R_{12} are the rates observed for the separate and combined sources. For simplicity also, let us assume that there is no background. In the non-extended case, we then have the relations

$$n_1 = \frac{R_1}{1-R_1\tau}, \quad n_2 = \frac{R_2}{1-R_2\tau} \quad \text{and}$$
$$n_1 + n_2 = \frac{R_{12}}{1-R_{12}\tau}. \tag{5.18}$$

Eliminating the n's, we have

$$\frac{R_{12}}{1-R_{12}\tau} = \frac{R_1}{1-R_1\tau} + \frac{R_2}{1-R_2\tau} \tag{5.19}$$

which yields the solution

$$\tau = \frac{R_1R_2 - [R_1R_2(R_{12}-R_1)(R_{12}-R_2)]^{1/2}}{R_1R_2R_{12}} . \tag{5.20}$$

While conceptually the double source method is quite simple, it is in practice, a cumbersome and time consuming method which yields results to no better than 5–10% [5.3]. This can be seen already in (5.20) which shows τ to be given by a difference between two numbers. From the point of view of statistical errors (see Sect. 4.6.1), of course, this is disadvantageous. Experimentally, care must also be taken to ensure the same positioning for the sources when they are measured separately and together. Even then, however, there may be scattering effects of one source on the other which may modify the combined rates, etc.

A number of other methods have been proposed, however. One technique is to replace one of the sources with a pulse generator [5.5] of frequency $f < (3\tau)^{-1}$. If R_s is the observed rate of the source alone and R_c is the observed combined rate of the source and generator, then it can be shown that the dead time in the non-extended case is

$$\tau \simeq \frac{1 - [(R_c - R_s)/f]^{1/2}}{R_s} . \tag{5.21}$$

Equation (5.21) is only approximate, but it should give results to better than 1% as long as the oscillator frequency condition stated above is met [5.3]. This method, of course, avoids the problem of maintaining a fixed source geometry but it does require an estimate of the dead time and a fast pulser to ensure the frequency condition above. A more general formula valid at all frequencies has been worked out by *Muller* [5.6] requiring, however, a long numerical calculation of a correction factor.

For an extended dead time, it can also be shown [5.3] that

$$(m + f - mf\tau)\exp(-m\tau) = R_c \tag{5.22}$$

where m is the true rate of the source. If (5.17) for the case of source alone is used, the relation

$$\frac{R_c - R_s}{f} = (1 - m\tau)\exp(-m\tau) \tag{5.23}$$

is found which can be solved for $m\tau$. If m is known then, of course, τ follows.

A very quick and accurate method which can be used for measuring the dead time of the electronics system alone is to inject pulses from two oscillators [5.3] of frequency f_1 and f_2 and to measure the mean frequency of the combined pulses, f_c. For the non-extended model, it can be shown then,

$$f_c = \begin{cases} f_1 + f_2 - 2f_1f_2\tau & \text{for} \quad 0 < \tau < T/2 \\ 1/T & \text{for} \quad T/2 < \tau < T \end{cases} \tag{5.24}$$

where T is the period of the faster oscillator, i.e., the smaller of $1/f_1$ and $1/f_2$. For the extended model, we have similarly

$$f_c = \begin{cases} f_1 + f_2 - 2f_1f_2\tau & \text{for} \quad 0 < \tau < T \\ 0 & \text{for} \quad \tau > T . \end{cases} \tag{5.25}$$

The expressions are thus identical if the frequency of the faster oscillator is chosen such that $f<(2\tau)^{-1}$; the dead time, *irrespective* of the model, is then given by

$$\tau=\frac{t_m}{2}\,\frac{R_1+R_2-R_c}{R_1R_2} \tag{5.26}$$

where R_1, R_2 and R_c are the total measured counts for the two oscillators separately and combined in a measurement period t_m. If f is chosen greater then $(2\tau)^{-1}$, then a determination of the model type can be made by comparing the results to the predictions in (5.24) and (5.25).

When using this method, of course, it is important to assure that the form of the pulses are close to those of true detector signals and that the frequencies of the oscillators are stable. In such cases, the two-oscillator method can yield quick and accurate results to a precision better than 10^{-3}.

10. Semiconductor Detectors

Semiconductor detectors, as their name implies, are based on crystalline semiconductor materials, most notably silicon and germanium. These detectors are also referred to as *solid-state* detectors, which is a somewhat older term recalling the era when *solid-state* devices first began appearing in electronic circuits. While work on crystal detectors was performed as early as the 1930's [10.1], real development of these instruments first began in the late 1950's The first prototypes quickly progressed to working status and commercial availability in the 1960's. These devices provided the first high-resolution detectors for energy measurement and were quickly adopted in nuclear physics research for charged particle detection and gamma spectroscopy. In more recent years, however, semiconductor devices have also gained a good deal of attention in the high energy physics domain as possible high-resolution particle track detectors. Much work is being put into developing these instruments [10.2, 3], along with gas detectors, as *the* detectors for the next generation of high energy experiments.

The basic operating principle of semiconductor detectors is analogous to gas ionization devices. Instead of a gas, however, the medium is now a solid semiconductor material. The passage of ionizing radiation creates electron-hole pairs (instead of electron-ion pairs) which are then collected by an electric field. The advantage of the semiconductor, however, is that the average energy required to create an electron-hole pair is some 10 times smaller than that required for gas ionization. Thus the amount of ionization produced for a given energy is an order of magnitude greater resulting in increased energy resolution. Moreover, because of their greater density, they have a greater stopping power than gas detectors. They are compact in size and can have very fast response times. Except for silicon, however, semiconductors generally require cooling to low temperatures before they can be operated. This, of course, implies an additional cryogenic system which adds to detector overhead One of the problems in current semiconductor detector research, in fact, is to find and develop new materials which can be operated at room temperature. Being crystalline materials, they also have a greater sensitivity to radiation damage which limits their long term use.

We will survey, in this chapter, the different types of semiconductor detectors and their operation. Since an understanding of these detectors requires some knowledge of solid-state physics, however, we shall also review some of the basic physics aspects of semiconductors and in particular semiconductor junctions. A more thorough discussion can be found in some of the standard texts on solid state physics given in the bibliography.

10.1 Basic Semiconductor Properties

In this section, we will briefly review the basic properties of semiconductor materials and those electrical characteristics which are important for their use as radiation detec-

tors. Our discussion here will be concerned with pure semiconductors which are also known as *intrinsic* semiconductors. The term "*pure*" here is relative, since in reality, no semiconductor is ever completely free of impurities in the lattice. For discussion purposes, however, we will assume that this is the case. Impurities, nevertheless, play an important role and may limit or enhance the characteristics of the material Their effects will be discussed in a later section.

10.1.1 Energy Band Structure

Semiconductors are crystalline materials whose outer shell atomic levels exhibit an *energy band* structure. Figure 10 1 schematically illustrates this basic structure consisting of a *valence* band, a *"forbidden" energy gap* and a *conduction* band. The band configuration for conductors and insulators are also shown for comparison

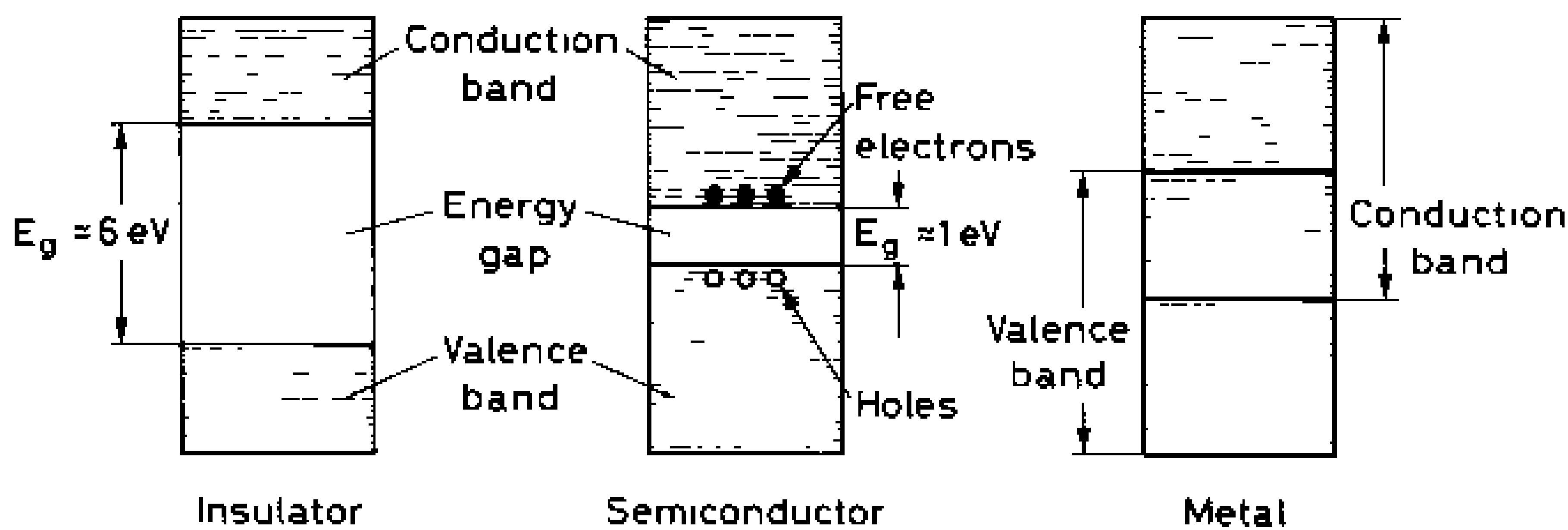

Fig. 10.1. Energy band structure of conductors, insulators and semiconductors

The *energy bands* are actually regions of many discrete levels which are so closely spaced that they may be considered as a continuum, while the *"forbidden"* energy gap is a region in which there are no available energy levels at all. This band structure arises because of the close, periodic arrangement of the atoms in the crystal which causes an overlapping of the electron wavefunctions. Since the Pauli principle forbids more than one electron in the same state, the degeneracy in the outer atomic shell energy levels breaks to form many discrete levels only slightly separated from each other. As two electrons of opposite spin may reside in the same level, there are as many levels as there are pairs of electrons in the crystal. This degeneracy breaking does not affect the inner atomic levels, however, which are more tightly bound.

The highest energy band is the conduction band. Electrons in this region are detached from their parent atoms and are free to roam about the entire crystal. The electrons in the valence band levels, however, are more tightly bound and remain associated to their respective lattice atoms.

The width of the gap and bands is determined by the lattice spacing between the atoms. These parameters are thus dependent on the temperature and the pressure. In conductors, the energy gap is nonexistent, while in insulators the gap is large. At normal temperatures, the electrons in an insulator are normally all in the valence band, thermal energy being insufficient to excite electrons across this gap. When an external electric field is applied, therefore, there is no movement of electrons through the crystal and thus no current. For a conductor, on the other hand, the absence of a gap makes it very easy for thermally excited electrons to jump into the conduction band where they are free to move about the crystal. A current will then flow when an electric field is ap-

plied. In a semiconductor, the energy gap is intermediate in size such that only a few electrons are excited into the conduction band by thermal energy. When an electric field is applied, therefore, a small current is observed. If the semiconductor is cooled, however, almost all the electrons will fall into the valence band and the conductivity of the semiconductor will decrease.

10.1.2 Charge Carriers in Semiconductors

At 0 K, in the lowest energy state of the semiconductor, the electrons in the valence band all participate in covalent bonding between the lattice atoms. This is illustrated in Fig. 10.2 for silicon and germanium. Both silicon and germanium have four valence electrons so that four covalent bonds are formed. At normal temperatures, however, the action of thermal energy can excite a valence electron into the conduction band leaving a *hole* in its original position. In this state, it is easy for a neighboring valence electron to jump from its bond to fill the hole. This now leaves a hole in the neighboring position. If now the next neighboring electron repeats the sequence and so on, the hole appears to move through the crystal. Since the hole is positive relative to the sea of negative electrons in the valence band, the hole acts like a positive charge carrier and its movement through the crystal also constitutes an electric current. In a semiconductor, the electric current thus arises from two sources: the movement of free electrons in the conduction band and the movement of holes in the valence band. This is to be contrasted with a metal where the current is carried by electrons only.

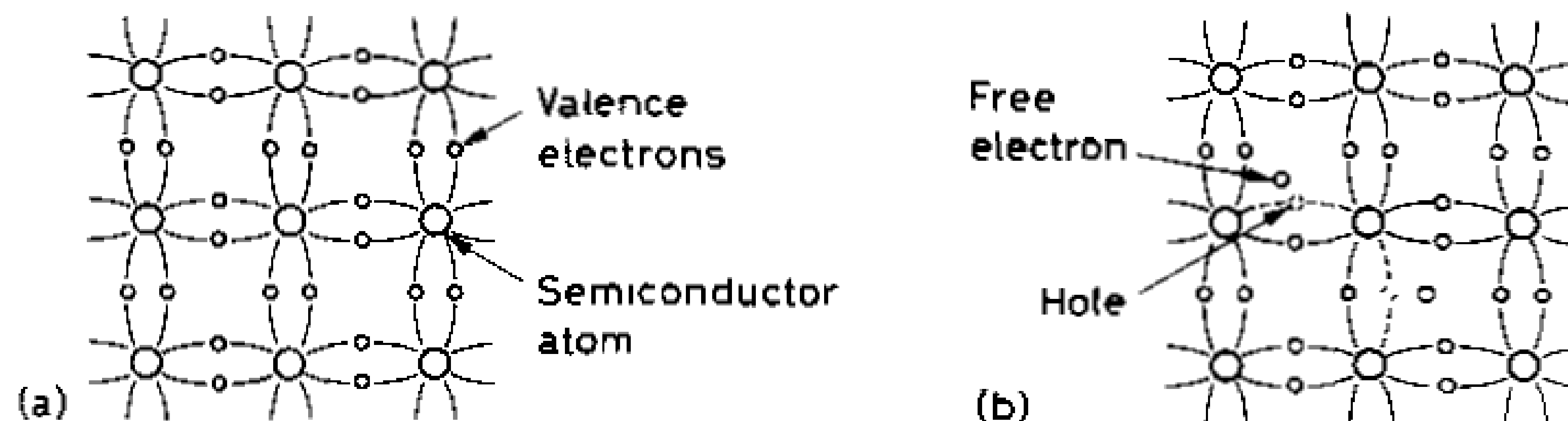

Fig. 10.2. Covalent bonding of silicon (**a**) at 0 K, all electrons participate in bonding, (**b**) at higher temperatures some bonds are broken by thermal energy leaving a *hole* in the valence band

10.1.3 Intrinsic Charge Carrier Concentration

In a semiconductor, electron-hole pairs are constantly being generated by thermal energy. At the same time, there are also a certain number of electrons and holes which recombine. Under stable conditions, an equilibrium concentration of electron-hole pairs is established. If n_i is the concentration of electrons (or equally holes) and T the temperature, then

$$n_i = \sqrt{N_c N_v}\, \exp\left(\frac{-E_g}{2kT}\right) = AT^{3/2} \exp\left(\frac{-E_g}{2kT}\right) , \tag{10.1}$$

where N_c is the number of states in the conduction band, N_v the number of states in the valence band, E_g the energy gap at 0 K and k the Boltzmann constant. N_c and N_v can be calculated from Fermi-Dirac statistics and each can be shown to vary as $T^{3/2}$. Making

this dependence explicit then gives the right-hand side of (10.1) where the constant A is independent of temperature.

Typical values for n_i are on the order of $2.5 \times 10^{13}\,\mathrm{cm}^{-3}$ for Ge and $1.5 \times 10^{10}\,\mathrm{cm}^{-3}$ for Si at $T = 300$ K. This should be put into perspective, however, by noting that there are on the order of 10^{22} atoms/cm^3 in these materials. This means that only 1 in 10^9 germanium atoms is ionized and 1 in 10^{12} in silicon! Despite the large exponents, therefore, the concentrations are very low.

10.1.4 Mobility

Under the action of an externally applied electric field, the drift velocity of the electrons and holes through a semiconductor can be written as

$$v_e = \mu_e E$$
$$v_h = \mu_h E \ , \tag{10.2}$$

where E is the magnitude of the electric field and μ_e and μ_h are the *mobilities* of the electrons and holes respectively. For a given material, the mobilities are functions of E and the temperature T. For silicon at normal temperatures [10.4], μ_e and μ_h are constant (Table 10.1) for $E < 10^3$ V/cm, so that the relation between velocity and E is linear. For E between $10^3 - 10^4$ V/cm, μ varies approximately as $E^{-1/2}$, while above 10^4 V/cm, μ varies as $1/E$. At this point the velocity saturates approaching a constant value of about 10^7 cm/s. Physically, saturation occurs because a proportional fraction of the kinetic energy acquired by the electrons and holes is drained by collisions with the lattice atoms.

Table 10.1. Some physical properties of silicon and germanium

	Si	Ge
Atomic number Z	14	32
Atomic weight A	28.1	72.6
Density [g/cm^2]	2.33	5.32
Dielectric constant (relative)	12	16
Intrinsic resistivity (300 K) [Ωcm]	230000	45
Energy gap (300 K) [eV]	1.1	0.7
Energy gap (0 K) [eV]	1.21	0.785
Electron mobility (300 K) [cm^2/Vs]	1350	3900
Hole mobility (300 K) [cm^2/Vs]	480	1900

At temperatures between 100 and 400 K, μ also varies approximately as T^{-m}, where m depends on the type of material and on the charge carrier. Values of m in silicon are $m = 2.5$ for electrons and $m = 2.7$ for holes, while in germanium, $m = 1.66$ for electrons and $m = 2.33$ for holes [10.4]. Measured values of the drift velocity as a function of T and E are given in [10.5].

The mobilities, of course, determine the current in a semiconductor. Since the current density $J = \rho v$, where ρ is the charge density and v the velocity, J in a pure semiconductor is given by

$$J = e n_i (\mu_e + \mu_h) E \ , \tag{10.3}$$

where we have substituted (10.2) for v and used the fact that current is carried by both electrons and holes. Moreover, $J = \sigma E$, where σ is the conductivity; comparison with (10.3), therefore, gives us the relation

$$\sigma = e n_i (\mu_e + \mu_h) \quad . \tag{10.4}$$

This also gives us the resistivity which is just the inverse of σ.

10.1.5 Recombination and Trapping

An electron may recombine with a hole by dropping from the conduction band into an open level in the valence band with the emission of a photon. This process is known as direct *recombination* and is the exact opposite of electron-hole generation. Since both momentum and energy are conserved, however, the electron and the hole must have exactly the right values in order for this to occur. Such processes are therefore very rare and indeed theoretical calculations [10.6] show that electrons and holes should have lifetimes as long as a second if this were the only process. Experimental measurements, however, show carrier lifetimes to range from nanoseconds to hundreds of microseconds which clearly implies that other mechanisms are involved.

The most important mechanism is through *recombination centers* resulting from impurities in the crystal. These elements perturb the energy band structure by adding additional levels to the middle of the forbidden energy gap as shown in Fig. 10.3. These states may capture an electron from the conduction band and then do one of two things: (1) after a certain holding time, the electron is released back into the conduction band, or, (2) during the holding time, it may also capture a hole which then annihilates with the trapped electron. Such centers are particularly efficient as the impurity is left in its original state so that each center may participate in many recombinations.

For radiation detection, the existence of recombination impurities plays a detrimental role since they will reduce the mean time charge carriers remain free. This time, of course, should be longer than the time it takes to collect the charges otherwise charge loss will occur with a subsequent reduction in resolution. Semiconductor detectors therefore require relatively pure crystals. For large volume detectors, in particular, the impurity concentration cannot be more than 10^{10} impurities per cm^3 [10.7].

A second effect which arises from impurities is *trapping*. Some impurities, in fact, are only capable of capturing one kind of charge carrier, that is electrons or holes, but not both. Such centers simply hold the electron or hole and then release it after a certain characteristic time. If the trapping time is on the order of the charge collection time, then quite obviously charges will be lost and incomplete charge collection will result. If the trapping time is very much smaller, then little or no effect occurs. Recombination centers are also trapping centers as we have seen.

While impurities are the principal source of recombination and trapping, structural defects in the lattice may also give rise to similar states in the forbidden band. Such de-

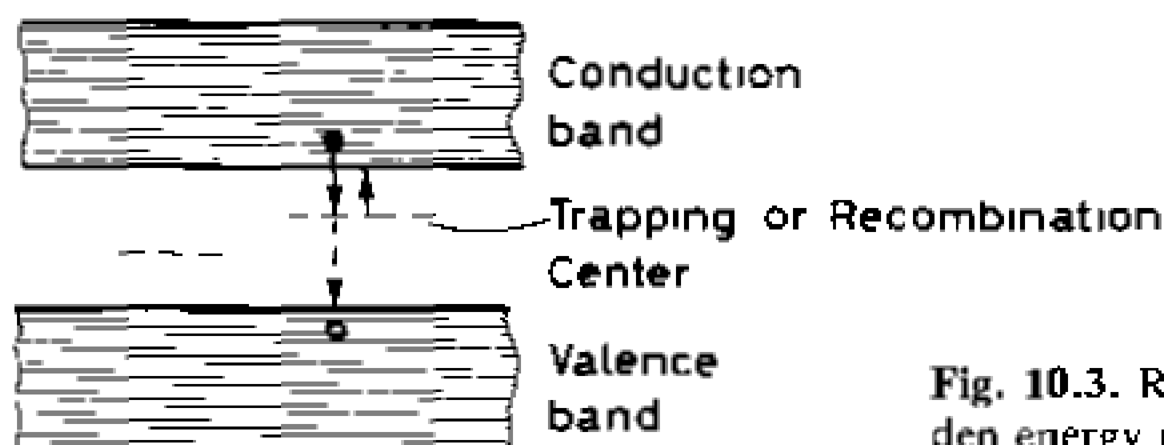

Fig. 10.3. Recombination and trapping sites in the forbidden energy gap

fects include simple *point* defects such as vacancies in the lattice or atoms which occupy positions in between lattice points, and *dislocations*, in which an entire line of atoms is displaced. These structural defects may arise during growth of the crystal or may be caused by thermal shock, plastic deformation, stress and bombardment by radiation. The latter source, of course, is of particular concern for detectors and is discussed in a later section.

While we have thus far discussed the detrimental effects of impurities, the addition of certain elements to pure semiconductors may also enhance the characteristics of the material. This is discussed in the next section on doped semiconductors. The difference between these impurities and recombination and trapping impurities is in the depth of the energy levels created in the forbidden band. As we will see, doping impurities create *shallow* levels very close to the conduction or valence bands, whereas recombination and trapping impurities produce *deep* levels near the center. Electrons and holes in shallow levels are easily excited out into the conduction and valence bands and thus are not trapped for very long periods.

10.2 Doped Semiconductors

In a pure semiconductor crystal, the number of holes equals the number of electrons in the conduction band. This balance can be changed by introducing a small amount of impurity atoms having one more or one less valence electron in their outer atomic shell. For silicon and germanium which are tetravalent, this means either pentavalent atoms or trivalent atoms. These impurities integrate themselves into the crystal lattice to create what are called *doped* or *extrinsic* semiconductors.

If the dopant is pentavalent, the situation in Fig. 10.4a arises. In the ground state, the electrons fill up the valence band which contains just enough room for four valence electrons per atom. Since the impurity atom has five valence electrons, an extra elec-

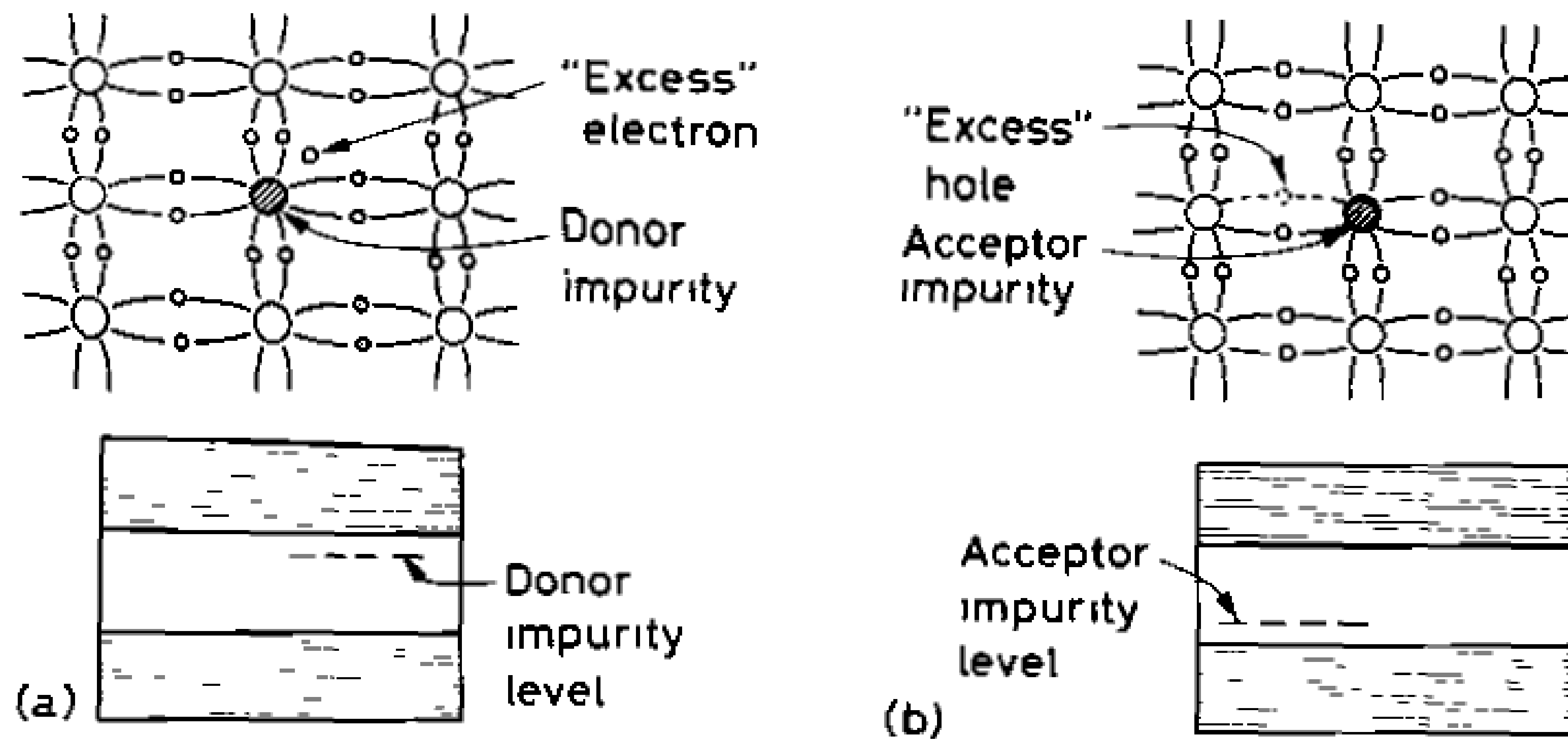

Fig. 10.4. (a) Addition of donor impurities to form n-type semiconductor materials. The impurities add *excess* electrons to the crystal and create donor impurity levels in the energy gap. **(b)** Addition of acceptor impurities to create p-type material. Acceptor impurities create an *excess* of holes and impurity levels close to the valence band

tron is left which does not fit into this band[1]. This electron resides in a discrete energy level created in the energy gap by the presence of the impurity atoms. Unlike recombination and trapping states, this level is extremely close to the conduction band being separated by only 0.01 eV in germanium and 0.05 eV in silicon. At normal temperatures, therefore, the *extra* electron is easily excited into the conduction band where it will enhance the conductivity of the semiconductor. In addition, the extra electrons will also fill up holes which normally form, thereby decreasing the normal hole concentration. In such materials, then, the current is mainly due to the movement of electrons. Holes, of course, still contribute to the current but only as *minority carriers*. Doped semiconductors in which electrons are the majority charge carriers are called *n-type* semiconductors.

If the impurity is now trivalent with one less valence electron, there will not be enough electrons to fill the valence band. There is thus an *excess* of holes in the crystal (Fig. 10.4b). The trivalent impurities also perturb the band structure by creating an additional state in the energy gap, but this time, close to the valence band as shown in Fig. 10.4b. Electrons in the valence band are then easily excited into this extra level, leaving extra holes behind. This excess of holes also decreases the normal concentration of free electrons, so that the holes become the majority charge carriers and the electrons minority carriers. Such materials are referred to as *p-type* semiconductors.

In practice, *donor* elements such as arsenic, phosphorous and antimony are used to make n-type semiconductors, while gallium, boron and indium are most often employed as *acceptor* impurities for p-type materials. The amount of dopant used is generally very small with typical concentrations being on the order of a few times 10^{13} atoms/cm^3. Since the densities of germanium and silicon are on the order of 10^{22} atoms/cm^3, this implies impurity concentrations of only a few parts per billion!

Great use is also made of heavily doped semiconductors particularly as the electrical contacts for semiconductors. Impurity concentrations in these materials can be as high as 10^{20} atoms/cm^3, so that they are highly conductive. To distinguish these semiconductors from normally doped materials, a "+" sign after the material type is used. A heavily doped p-type semiconductor is therefore written as p^+ and a heavily doped *n* semiconductor as n^+.

Regardless of the type of dopant, the concentration of electrons and holes obey a simple law of mass action when in thermal equilibrium. If n is the concentration of electrons and p is the concentration of holes, then their product is

$$np = n_i^2 = AT^3 \exp\left(\frac{-E_g}{kT}\right) , \tag{10.5}$$

where n_i is the intrinsic concentration given in (10.1). Since the semiconductor is neutral, the positive and negative charge densities must be equal, so that

$$N_D + p = N_A + n , \tag{10.6}$$

where N_D and N_A are the donor and acceptor concentrations. In an n-type material, where $N_A = 0$ and $n \gg p$, the electron density is therefore

$$n \simeq N_D , \tag{10.7}$$

[1] Note this extra electron does not imply that the crystal is now charged. Electrical neutrality is assured since the nucleus of the impurity atom also contains an *extra* positive proton.

i.e., the electron concentration is approximately the same as the dopant concentration. Using (10.5), then, the minority carrier concentration is

$$p \simeq \frac{n_i^2}{N_D} . \quad (10.8)$$

From (10.4), the conductivity or resistivity of an n-type material thus becomes

$$\frac{1}{\rho} = \sigma \simeq e N_D \mu_e . \quad (10.9)$$

An analogous result is found for p-type materials.

10.2.1 Compensation

A question one can ask now is what happens if both n- and p-type impurities are added to a semiconductor. In reality, all semiconductors do, in fact, contain impurities of both types. Since the extra electrons from donor atoms will be captured by extra holes from acceptor materials, it is easy to see that a cancellation effect occurs What counts, therefore, is the net concentration, $|N_D - N_A|$, where N_D and N_A are the concentrations of donor and acceptor atoms. If $N_D > N_A$, then the semiconductor is an n-type and vice-versa. Similarly, semiconductors with equal amounts of donor and acceptor impurities remain intrinsic or at least retain most of the characteristics of intrinsic materials. Such materials are known as *compensated* materials and are designated with the letter "*i*". (This should *not* be confused with *intrinsic*).

It is quite obviously difficult to make compensated materials because of the need to have *exactly* the same amounts of donor and acceptor impurities. The first breakthrough came in the 1960's when Pell developed the lithium drifting method for compensating p-type silicon and germanium. While we will not go into detail, the process consists essentially of diffusing lithium, which acts as a donor, onto the surface of a p-type material. This changes that end of the semiconductor into an n-type material. The concentration of lithium drops off in a Gaussian manner so that the junction between the n-type and p-type regions lies at some depth under the surface. A bias voltage is then applied across the junction such that the positive lithium ions are pulled further into the bulk of the p-region. To increase lithium mobility, the temperature of the material is raised. As the lithium donor concentration increases in the p-region, its concentration decreases in the n-region. Because of the dynamics of the local electric field, however, the donor concentration of the p-side cannot exceed the acceptor concentration and vice versa on the n-side. Indeed, if this happens the local field essentially reverses direction and sweeps the ions back in the opposite direction. An equilibrium point is thus reached in which the lithium donor ions spread themselves over a region such that the number of donors is exactly equal to the number of acceptors. A compensated region is thus formed. To obtain thick compensated regions from 10 – 15 mm, this drift process can take several days. The interested reader may find a more detailed description of the process in [10.8].

Because of the high mobility of the lithium ions at room temperature, particularly in germanium, it is necessary to cool the material to liquid nitrogen temperatures once the desired compensation is obtained. This temperature must be maintained at all times in order to preserve the compensation. In the case of silicon, however, lithium mobility is lower so that short periods at room temperature usually do no harm

The most important property of compensated material is its high resistivity. Rough measurements on silicon have yielded values as high as 100000 Ω cm. This is still much lower than the intrinsic maximum value of ~230000 Ω cm, however, so that although the drifting process is effective, it is still not perfect. We will see how these materials are used for radiation detection in Sects. 10.5.4 and 10.7.1.

10.3 The np Semiconductor Junction. Depletion Depth

The functioning of all present-day semiconductor detectors depends on the formation of a semiconductor *junction*. Such junctions are better known in electronics as rectifying diodes, although that is not how they are used as detectors. Semiconductor diodes can be formed in a number of ways. A simple configuration which we will use for illustration purposes is the pn junction formed by the juxtaposition of a p-type semiconductor with an n-type material. These junctions, of course, cannot be obtained by simply pressing n- and p-type materials together. Special techniques must be used instead to achieve the intimate contact necessary for junction formation. One method, for example, is to diffuse sufficient p-type impurities into one end of a homogeneous bar of n-type material so as to change that end into a p-type semiconductor. Others methods are also available and will be discussed in later sections.

The formation of a pn-junction creates a special zone about the interface between the two materials. This is illustrated in Fig. 10.5. Because of the difference in the concentration of electrons and holes between the two materials, there is an initial diffusion of holes towards the n-region and a similar diffusion of electrons towards the p region. As a consequence, the diffusing electrons fill up holes in the p-region while the diffusing holes capture electrons on the n-side. Recalling that the n and p structures are initially neutral, this recombination of electrons and holes also causes a charge build-up to occur on either side of the junction. Since the p-region is injected with extra electrons it thus becomes negative while the n-region becomes positive. This creates an electric field gradient across the junction which eventually halts the diffusion process leaving a region of immobile space charge. The charge density and the corresponding electric field profile are schematically diagrammed in Fig. 10.5 Because of the electric field, there is a potential difference across the junction. This is known as the *contact* potential. The

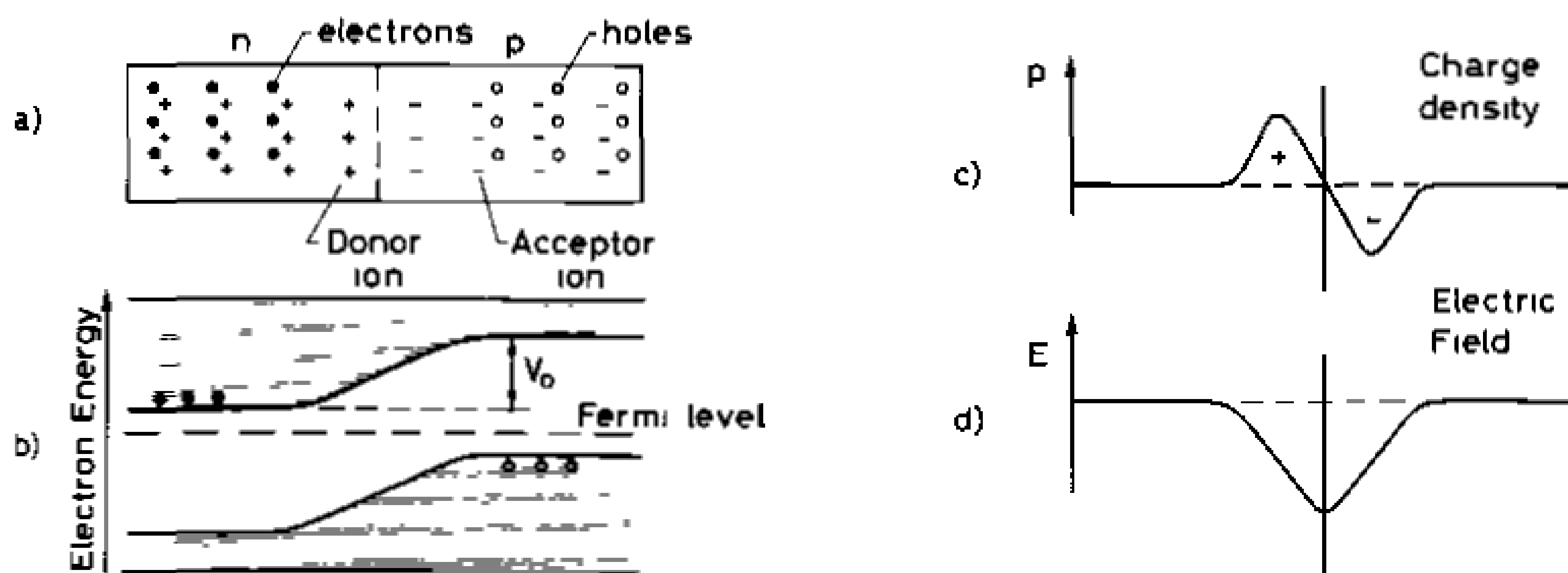

Fig. 10.5. (a) Schematic diagram of an np junction, **(b)** diagram of *electron* energy levels showing creation of a contact potential V_0, **(c)** charge density, **(d)** electric field intensity

energy band structure is thus deformed as shown in Fig. 10.5, with the contact potential generally being on the order of 1 V.

The region of changing potential is known as the *depletion* zone or *space charge region* and has the special property of being devoid of all mobile charge carriers. And, in fact, any electron or hole created or entering into this zone will be swept out by the electric field. This characteristic of the depletion zone is particularly attractive for radiation detection. Ionizing radiation entering this zone will liberate electron-hole pairs which are then swept out by the electric field. If electrical contacts are placed on either end of the junction device, a current signal proportional to the ionization will then be detected. The analogy to an ionization chamber thus becomes apparent.

10.3.1 The Depletion Depth

The width of the depletion zone is generally small and depends on the concentration of n and p impurities. If the charge density distribution in the zone, $\rho(x)$ is known, this can be determined from Poisson's equation,

$$\frac{d^2V}{dx^2} = -\frac{\rho(x)}{\varepsilon} \ , \tag{10.10}$$

where ε is the dielectric constant.

As an illustration, let us take the simple example of a uniform charge distribution about the junction [10.9]. This is illustrated in Fig. 10.6. Letting x_n denote the extent of the depletion zone on the n-side and x_p the depth on the p-side, we then have,

$$\rho(x) = \begin{cases} eN_D & 0 < x < x_n \\ -eN_A & -x_p < x < 0 \ , \end{cases} \tag{10.11}$$

where e is the charge of the electron and N_D and N_A are the donor and acceptor impurity concentrations Since the total charge is conserved, we also have the relation

$$N_A x_p = N_D x_n \ . \tag{10.12}$$

Now integrating (10.10) once, we find

$$\frac{dV}{dx} = \begin{cases} -\dfrac{eN_D}{\varepsilon}x + C_n & 0 < x < x_n \\ \dfrac{eN_A}{\varepsilon}x + C_p & -x_p < x < 0 \ , \end{cases} \tag{10.13}$$

where C_n and C_p are integration constants. Since $dV/dx = 0$ at $x = x_n$ and $-x_p$, (10.13) becomes

$$\frac{dV}{dx} = \begin{cases} -\dfrac{eN_D}{\varepsilon}(x - x_n) & 0 < x < x_n \\ \dfrac{eN_A}{\varepsilon}(x + x_p) & -x_p < x < 0 \ . \end{cases} \tag{10.14}$$

Equation (10.14), of course, represents the electric field in the space charge region. One more integration now yields,

$$V(x) = \begin{cases} -\dfrac{eN_D}{\varepsilon}\left(\dfrac{x^2}{2} - x_n x\right) + C & 0 < x < x_n \\ \dfrac{eN_A}{\varepsilon}\left(\dfrac{x^2}{2} + x_p x\right) + C' & -x_p < x < 0 \ . \end{cases} \tag{10.15}$$

Since the two solutions must join at $x = 0$, it is clear that $C = C'$. Now at $x = x_n$, $V(x) = V_0$ which is the contact potential; thus

$$V_0 = \frac{eN_D}{2\varepsilon} x_n^2 + C \ . \tag{10.16}$$

Similarly on the p-side $V = 0$ at $x = -x_p$, so that

$$0 = -\frac{eN_A}{2\,\varepsilon} x_p^2 + C \ . \tag{10.17}$$

Eliminating C, we then obtain

$$V_0 = \frac{e}{2\,\varepsilon}(N_D x_n^2 + N_A x_p^2) \ . \tag{10.18}$$

Using (10 12) then yields,

$$x_n = \left(\frac{2\,\varepsilon V_0}{eN_D(1 + N_D/N_A)}\right)^{1/2} \ , \quad x_p = \left(\frac{2\,\varepsilon V_0}{eN_A(1 + N_A/N_D)}\right)^{1/2} \tag{10.19}$$

From (10.19), we can see that if one side is more heavily doped than the other, which is usually the case, then the depletion zone will extend farther into the lighter-doped side For example, if $N_A \gg N_D$, then $x_n \gg x_p$ which means that the depletion region is almost entirely on the n-side of the junction.

The total width of the depletion zone can now be easily found

$$d = x_n + x_p = \left(\frac{2\,\varepsilon V_0}{e}\,\frac{(N_A + N_D)}{N_A N_D}\right)^{1/2} \ . \tag{10.20}$$

If $N_A \gg N_D$, as in our example above, then (10.20) is approximately,

$$d \simeq x_n \simeq \left(\frac{2\,\varepsilon V_0}{eN_D}\right)^{1/2} \tag{10.21}$$

Using the expression in (10.9) for the resistivity ρ, (10.21) can be expressed as

$$d \simeq (2\,\varepsilon \rho_n \mu_e V_0)^{1/2} \ , \tag{10.22}$$

where ρ_n is the resistivity of the n-region. For the case of a heavily doped n-side ($N_D \gg N_A$), the depletion region will be entirely on the p-side, so that the factor $\rho_n \mu_e$ in (10.22) should be replaced by $\rho_p \mu_h$. Evaluating some of the constants now, we find the formulae

Silicon

$$d \simeq \begin{cases} 0.53(\rho_n V_0)^{1/2}\ \mu\mathrm{m} & \text{n-type} \\ 0.32(\rho_p V_0)^{1/2}\ \mu\mathrm{m} & \text{p-type} \end{cases}$$

Germanium (10.23)

$$d \simeq \begin{cases} (\rho_n V_0)^{1/2}\ \mu\mathrm{m} & \text{n-type} \\ 0.65(\rho_p V_0)^{1/2}\ \mu\mathrm{m} & \text{p-type} \end{cases}$$

where ρ is in Ω cm and V_0 in Volts. If we take typical values of $\rho \sim 20000\ \Omega$ cm for high-resistivity n-type silicon and $V_0 = 1$ V, this yields $d \simeq 75\ \mu$m, which is a rather small sensitive depth.

10.3.2 Junction Capacitance

Because of its electrical configuration, the depletion layer also has a certain capacitance which, as we will see later, affects the noise characteristics when the junction is used as a detector. For a planar geometry, the capacitance is

$$C = \varepsilon \frac{A}{d} , \tag{10.24}$$

where A is the area of the depletion zone and d its width. Substituting in the formulae of (10.23) then yields

Silicon

$$C/A = \begin{cases} 2.2(\rho_n V_0)^{-1/2}\ \mathrm{pF/mm^2} & \text{n-type} \\ 3.7(\rho_p V_0)^{-1/2}\ \mathrm{pF/mm^2} & \text{p-type} \end{cases}$$

Germanium (10.25)

$$C/A = \begin{cases} 1.37(\rho_n V_0)^{-1/2}\ \mathrm{pF/mm^2} & \text{n-type} \\ 2.12(\rho_p V_0)^{-1/2}\ \mathrm{pF/mm^2} & \text{p-type} \end{cases}$$

10.3.3 Reversed Bias Junctions

While the pn-junction described above will work as a detector, it does not present the best operating characteristics. In general, the intrinsic electric field will not be intense enough to provide efficient charge collection and the thickness of the depletion zone will be sufficient for stopping only the lowest energy particles. As we will see later, this small thickness also presents a large capacitance to the electronics and increases noise in the signal output. Better results can be obtained by applying a reverse-bias voltage to the junction, i.e., a negative voltage to the p-side, as shown in Fig. 10.7. This voltage will have the effect of attracting the holes in the p-region away from the junction and towards the p contact and similarly for the electrons in the n-region. The net effect is to

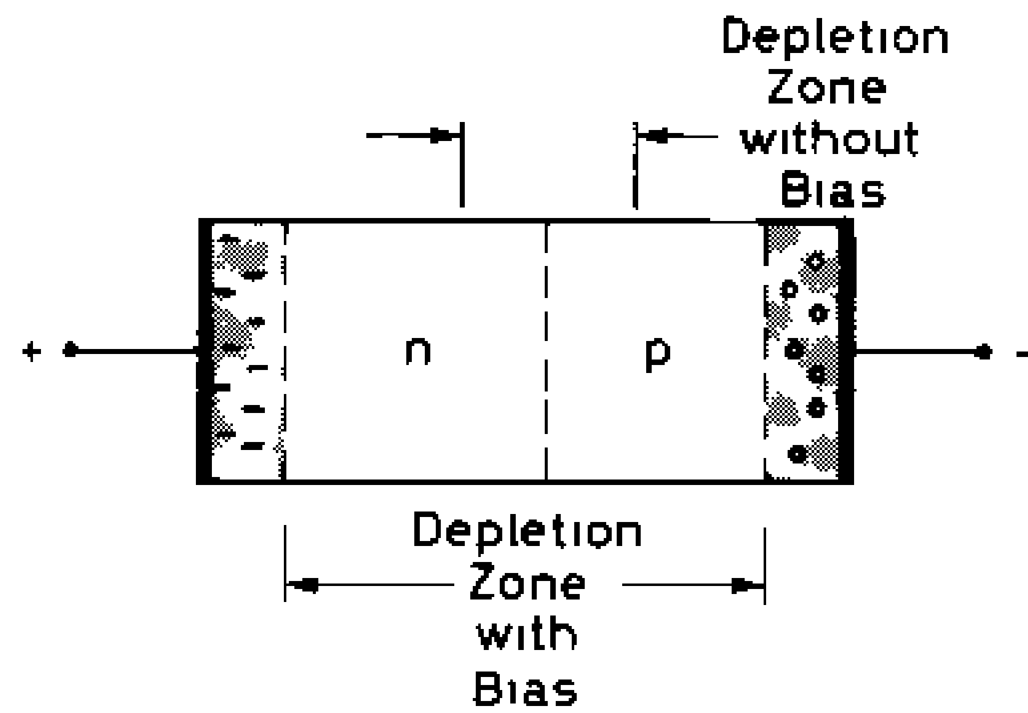

Fig. 10.7. Reversed bias junction

enlarge the depletion zone and thus the sensitive volume for radiation detection – the higher the external voltage, the wider the depletion zone. Moreover, the higher external voltage will also provide a more efficient charge collection. The maximum voltage which can be applied, however, is limited by the resistance of the semiconductor. At some point, the junction will breakdown and begin conducting.

Under a reverse bias, the width of the depletion layer can be calculated from (10.20) by replacing V_0 with $V_0 + V_B$, where V_B is the bias voltage. In general $V_0 \ll V_B$, so that V_0 may usually be neglected and equations (10.20) to (10.23) used directly with the substitution $V_0 \Rightarrow V_B$. This is also true for the capacitance in (10.25). An interesting point to note is that because of the difference in mobility between electrons and holes, the same bias voltage V_B will yield a somewhat larger depletion depth if the material is n-type rather than p-type.

If we now calculate the depth for n-type silicon, we can see that a depletion layer greater than 1 mm can be obtained if a reverse bias of about $V_B = 300$ V is applied. This, of course, is a great improvement over the few tens of microns in an unbiased junction. With current high resistivity silicon, depletion depths up to 5 mm can be obtained before breakdown occurs. In order to obtain greater depletion widths, even higher resistivity material is necessary which means using higher purity semiconductors or compensated material. These will be discussed in a later section.

10.4 Detector Characteristics of Semiconductors

Having reviewed some of the basic properties of semiconductor materials and junctions, we now turn to some of the characteristics of semiconductors as detectors of radiation.

Figure 10.8 shows the basic configuration used for operating a junction diode as a radiation detector. In order to be able to collect the charges produced by radiation, electrodes must be fitted onto the two sides of the junction. With semiconductors, however, an *ohmic* metal contact cannot, in general, be formed by directly depositing the metal onto the semiconductor material. Indeed, as we shall see in Sect. 10.5.2, contact between many metals and semiconductors results in the creation of a rectifying junction with a depletion zone extending into the semiconductor. To prevent this formation, a heavily doped layer of n^+ and p^+ material is used between the semiconductor and the metal leads. Because of the high dopant concentrations, the depletion depth is

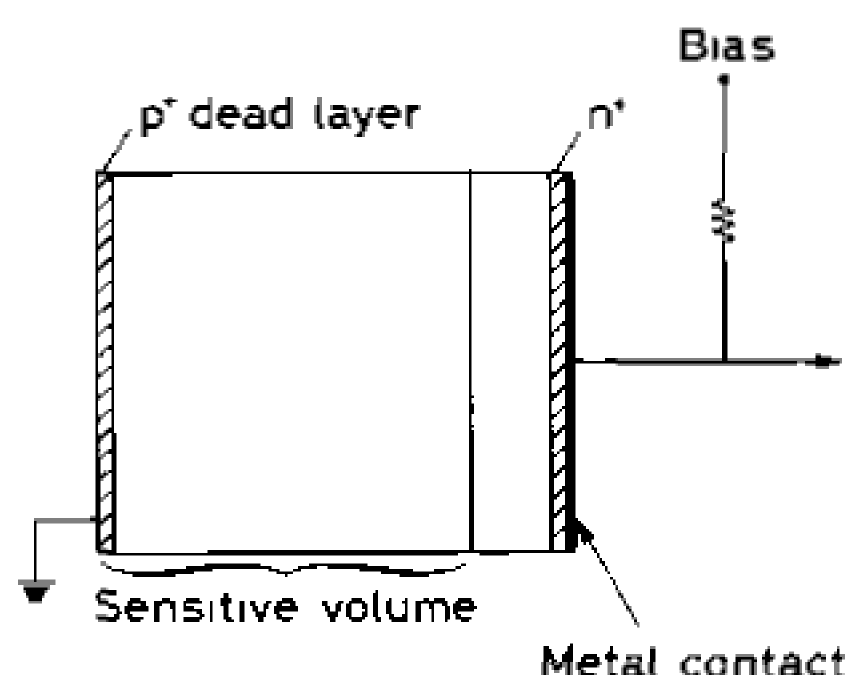

Fig. 10.8. Basic layout of a junction diode detector

then essentially zero as can be seen from (10.19). This then forms the desired *ohmic* contact.

For signal isolation purposes, the bias voltage to the detector is supplied through a series resistor rather than directly. To collect the charge signal from the detector, a preamplifier of the charge-sensitive type is generally used. Because of the low-level of the signal, this preamplifier must have low-noise characteristics. Signal processing after the preamplifier also requires pulse shaping in order to obtain the best signal-to-noise characteristics as explained in Chap. 14.

10.4.1 Average Energy per Electron-Hole Pair

The primary advantage of semiconductors over other detectors is the very small average energy needed to create an electron-hole pair. Like gases, the average energy at a given temperature is found to be independent of the type and energy of the radiation and only dependent on the type of material. Table 10.2 summarizes these values for various semiconductors at normal and liquid nitrogen temperatures.

Table 10.2 Average energy for electron hole creation in silicon and germanium

	Si	Ge
300 K	3.62 eV	–
77 K	3.81 eV	2.96 eV

For the same radiation energy, the number of charge carriers created will therefore be almost an order of magnitude greater in these materials than in gases. Compared to the number of photoelectrons created in a scintillation counter, this increase approaches two orders of magnitude. Not surprisingly, semiconductors should provide a greatly improved energy resolution.

As small as the average energies are it is interesting to compare these values to the band gaps in Table 10.1. Since the gaps are only on the order 1 eV wide, it is clear that less than a third of the energy deposited by passing radiation is actually spent on the production of electron-hole pairs. The other two thirds, in fact, go into exciting lattice vibrations.

10.4.2 Linearity

Assuming that the depletion region is sufficiently thick to completely stop all particles, the response of semiconductors should be perfectly linear with energy. If E is the energy of the radiation then E/w electron-hole pairs should be created, where w is the average energy from Table 10.2. Assuming a collection efficiency n, then a charge $Q = nE/w$ is collected on the electrodes. Since the depletion region has a capacitance C, as we saw in Sect. 10.3.2, the observed voltage on the electrodes is then

$$V = \frac{Q}{C} = n\frac{E}{wC} \qquad (10.26)$$

which varies linearly with E. Moreover, since w is independent of particle type, the response is, in principle, also independent of the type of radiation. This turns out to be true only for lightly ionizing radiation such as electrons and protons. For heavier ions, *plasma* effects occur which affect the collection efficiency and lead to differences in the pulse height between different particles with the same energy. This is discussed further in Sect. 10.9.5.

If the depletion zone is smaller than the range of the radiation, it is clear then that a nonlinear response should be expected since the full energy is not totally deposited in the sensitive volume. What is measured instead is the energy loss ΔE which is a nonlinear function of energy. For a given depletion depth, the response is therefore linear up until the range of the particles exceeds this depth.

10.4.3 The Fano Factor and Intrinsic Energy Resolution

The intrinsic energy resolution, as we saw in Chap. 5, is dependent on the number of charge carriers and the Fano Factor. Despite numerous experiments, the Fano factor for both silicon and germanium is still not well determined. However, it is clear that F is small and on the order of 0.12. This, of course, contributes greatly to enhancing the resolution of semiconductors which already profit greatly from the small average energy required to create an electron hole pair.

From (5.6), the expected resolution is

$$R = 2.35\sqrt{\frac{F}{J}} = 2.35\sqrt{\frac{Fw}{E}} \, , \qquad (10.27)$$

where w is the average energy for electron-hole creation and $J = E/w$. For a 5 MeV alpha particle, the intrinsic resolution expected for silicon is therefore $R \simeq 0.07\%$ or 3.5 keV. Typical measured resolutions are about 18 keV, however, which indicates that contributions from other sources, e.g., electronics, play important roles

10.4.4 Leakage Current

Although a reversed biased diode is ideally nonconducting, a small fluctuating current nevertheless flows through semiconductor junctions when voltage is applied. This current appears as noise at the detector output and sets a limit on the smallest signal pulse height which can be observed.

The leakage current has several sources. One is the movement of minority carriers, i.e., holes from the n-region which are attracted across the junction to the p-side and electrons from the p-region which are similarly attracted to the opposite side. This current is generally quite small and in the range of nanoamperes per cm^2. A second source is thermally generated electron-hole pairs originating from recombination and trapping enters in the depletion region. These centers cannot capture electrons or holes since they have all been swept out, but they can catalyze the creation of electrons and holes from the valence band by serving as intermediate states. The contribution from this source depends on the absolute number of traps in the depletion region and thus on their concentration and the volume of the zone. In general, current densities on the order of a few μA/cm^2 can be expected. The third and by far the largest source of leakage current is through surface channels. This component is complex and depends on very many factors including the surface chemistry, the existence of contaminants, the surrounding atmosphere, the type of mounting, etc. Clean encapsulation is generally required here to minimize this component.

10.4.5 Sensitivity and Intrinsic Efficiency

For charged particles, the intrinsic detection efficiency of semiconductors is close to 100% as very few particles will fail to create some ionization in the sensitive volume. The limiting factor on sensitivity is the noise from leakage currents in the detector and the associated electronics which set a lower limit on the pulse amplitude which can be detected. To ensure an adequate signal, the depletion depth must therefore be chosen sufficiently thick such that enough ionization will be produced to form a signal larger than the noise level. These events are then detected with almost 100% efficiency. If energy measurements are being made, however, the depletion depth must also be larger than the range of the particles. Figure 10.9 shows the range of various particles in silicon.

For gamma-ray detection, germanium is preferred over silicon because of its higher atomic number. However, because of the smaller band gap, the leakage current in germanium at normal temperatures is too high to be acceptable and must be cooled to liq-

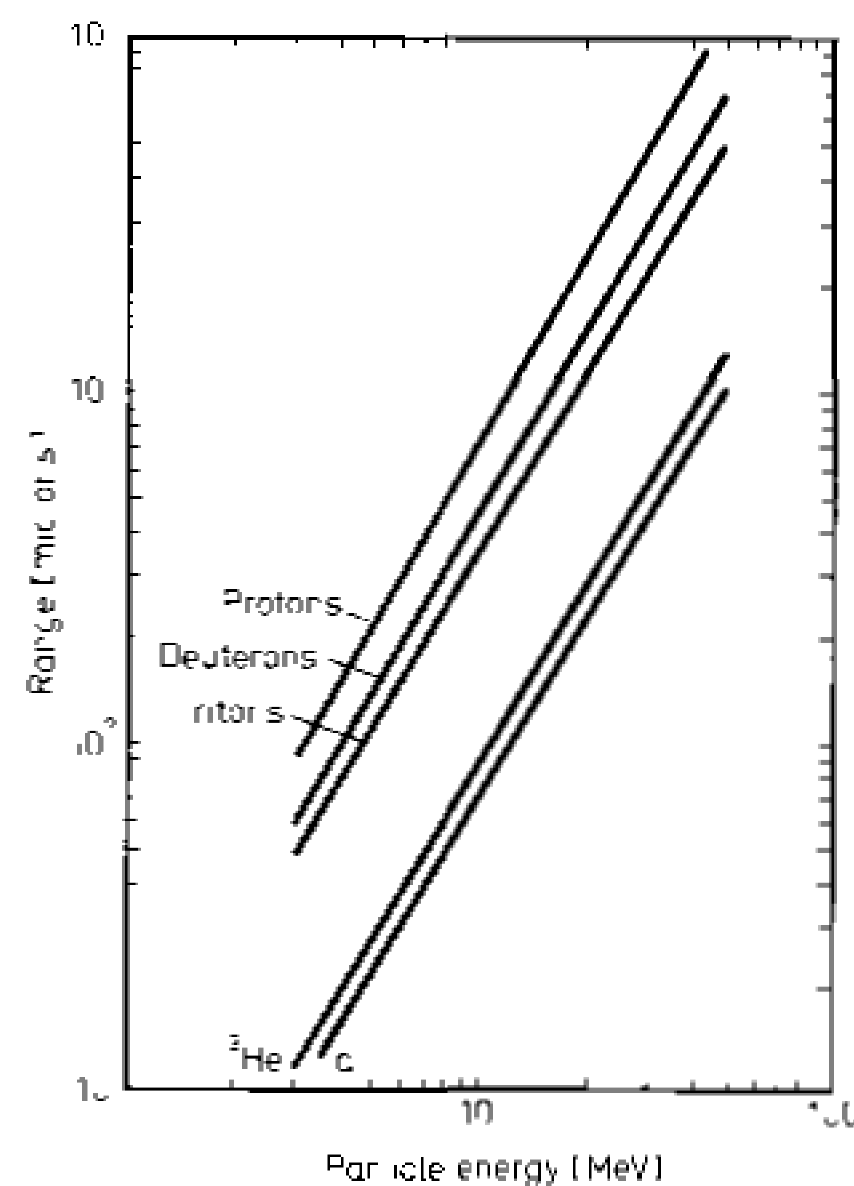

Fig. 10.9. Range of various particles in silicon (from *Skyrme* [10.10])

uid nitrogen temperatures. For low energy x-rays below ~30 keV, silicon detectors are preferred because of the K-edge in germanium which is located at ~11 keV. Photon absorption at these energies, of course, would yield almost zero energy photoelectrons.

10.4.6 Pulse Shape. Rise Time

Because the collection time for electrons and holes depends on the location of the charges with respect to the electrodes, pulse shapes from semiconductors vary in form and rise time.

As in gas detectors, the electrical pulse on the electrodes arises from induction caused by the movement of the charges rather than the actual collection of the charge itself. Assuming two parallel electrodes, (6.29) gives the change in potential energy for a charge q which moves a distance dx. Since we are interested in the charge collected we can reexpress this as

$$dQ = \frac{q\,dx}{d} , \tag{10.28}$$

where d is the distance between electrodes. Although (10.28) is derived for the case of empty space between the electrodes, it can be shown that this is also valid [10.11] in the presence of a space-charge as well.

Let us take the example of a pn-junction detector. These are generally formed from a p-type material which is heavily doped on one side with n-type donors. As we saw in Sect. 10.3.1, the depletion zone then extends almost entirely into the p-side This is illustrated in Fig 10.10 which also shows the electric field in the zone as given by (10.13). Using the coordinate system shown in the figure, (10.13) is rewritten as

$$E = -\frac{eN_A}{\varepsilon}x . \tag{10.29}$$

From (10.9), we have the result that the conductivity, $\sigma \simeq eN_A\mu_h$. Substituting into (10 29) then gives us

$$E = -\frac{x}{\mu_h \tau} , \tag{10.30}$$

where we have defined $\tau = \varepsilon/\sigma = \rho\varepsilon$ and ρ is the resistivity.

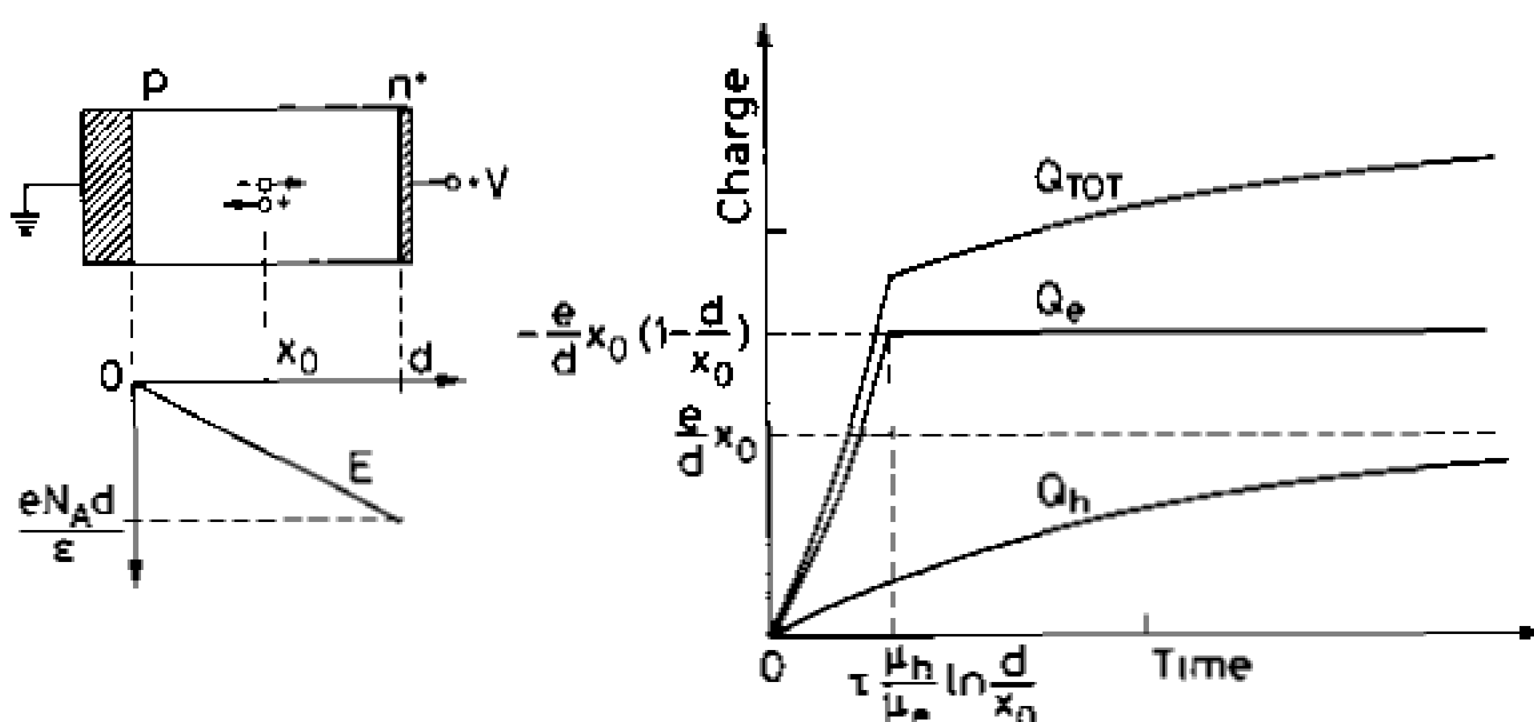

Fig. 10.10. Signal pulse shape due to a single electron hole pair in an np junction

Assume now that an electron-hole pair is created at a point x in the depletion zone. The electron will thus begin to drift towards the n^+ layer and the hole towards the p electrode. From the definition of mobility, we have for electrons

$$v = \frac{dx}{dt} = -\mu_e E = \frac{\mu_e}{\mu_h}\,\frac{x}{\tau} \ . \tag{10.31}$$

Assuming that the mobilities are independent of E, this yields the solution

$$x(t) = x_0 \exp\frac{\mu_e t}{\mu_h \tau} \ . \tag{10.32}$$

The time it takes for the electron to reach the electrode at $x = d$ is then

$$t = \tau\frac{\mu_h}{\mu_e}\ln\frac{d}{x_0} \ . \tag{10.33}$$

The charged induced as a function of t during this period is thus

$$Q_e(t) = -\frac{e}{d}\int\frac{dx}{dt}\,dt = \frac{e}{d}x_0\left(1-\exp\frac{\mu_e t}{\mu_h}\right) \ . \tag{10.34}$$

Similarly for the hole, we have the equation,

$$v_h = \frac{dx}{dt} = \mu_h E = -\frac{x}{\tau} \tag{10.35}$$

which yields the solution,

$$x(t) = x_0 \exp\frac{-t}{\tau} \ . \tag{10.36}$$

The collection time in this case is infinite and the induced charge,

$$Q_h(t) = -\frac{e}{d}x_0\int\exp\frac{-t}{\tau}\frac{dt}{\tau} = -\frac{e}{d}x_0\left(1-\exp\frac{-t}{\tau}\right) \ . \tag{10.37}$$

The pulse shape is now given by the total charge induced and this is diagrammed in Fig. 10.10 along with the contributions Q_e and Q_h. The total charge collected is $Q_{tot} = -e$ as can be shown by taking the maximum limits on (10.34) and (10.37).

The parameter τ, as can be seen, determines the rise time of the signal. In silicon, this is given roughly by $\tau = \rho \cdot 10^{-12}$ s, where ρ is in Ω cm. For typical 1000 Ω cm material, τ is thus on the order of a nanosecond.

The above calculation, of course, was only for a single electron-hole pair. To calculate the pulse shape due to incident radiation, it is necessary to know the particle trajectory, the density of ionization along the track, the variation of mobilities, the electric field distribution, etc. and integrate all these factors – a complicated task!

vides spatial information in a manner analogous to gas drift chambers. Tests with a prototype chamber [10.18] have shown a spatial resolution of 5 μm with minimum ionizing particles which is equivalent to that obtained with micro-strip detectors. The great advantage of these devices, of course, is the small volume of electronics required.

Some of the other new detectors proposed rely on the use of *charged-coupled devices* (CCD) These are silicon devices consisting of a two-dimensional array of tiny potential wells each covering a surface area of a few square microns. One chip contains tens of thousands of elements. When struck by radiation, electrons are released which are then trapped in these wells. This charge information is then readout by successively shifting the charge from one well to the next until it reaches the output electronics. A more detailed description of these detectors is given in [10.2, 19]. CCD's have been mainly used for light imaging purposes and are extremely sensitive, low noise devices. As a detector, spatial resolutions for these instruments are expected to be better than 2 μm However, they are very limited in counting rate. A review of these and other devices may also be found in the articles by *Charpak* and *Sauli* [10.2] and *Klanner* [10.20].

10.7 Germanium Detectors

For gamma-ray detection, germanium is preferred over silicon because of its much higher atomic number ($Z_{Si} = 14$, $Z_{Ge} = 32$). The photoelectric cross section is thus about 60 times greater in Ge than Si. Germanium, however, must be operated at low temperatures because of its smaller band gap. This inconvenience is offset, however, by its greater efficiency

Germanium may also be used for charged-particle detection, however, apart from its greater stopping power, it offers no advantage over silicon and, in fact, becomes disadvantageous because of its need for cooling.

10.7.1 Lithium-Drifted Germanium – Ge(Li)

In order to obtain a sufficient sensitive thickness for the detection of gamma rays, the first detectors were made from lithium compensated germanium. These detectors are known as Ge(Li) (pronounced as *jelly*) detectors. Since maximum obtainable thicknesses for compensated germanium are about 15 or 20 mm, a coaxial geometry is generally use to maximize the sensitive volume. This is schematically diagramed in Fig. 10.18. In this configuration, lithium is drifted in from the outer surface of a cylindrical crystal of p-type germanium to form a cylindrical shell of compensated material. A central core of insensitive p material is then left. If this core extends along the entire length of the axis, the configuration is then known as a *true coaxial* or *open-ended coaxial* detector. To increase sensitive volume even further, lithium may also be drifted in from the front face of the cylinder. The extent of the insensitive core is then reduced. These are known as *closed-end* coaxial detectors. For high counting efficiency, the central core may also be removed to form a *well type* detector. The various configurations are illustrated in Fig. 10.18. For lower gamma energies, Ge(Li) detectors may also be fabricated with the conventional planar geometry.

Because of the high mobility of the lithium ions in germanium, even at room temperature, Ge(Li) detectors must be kept at liquid nitrogen temperatures at all times.

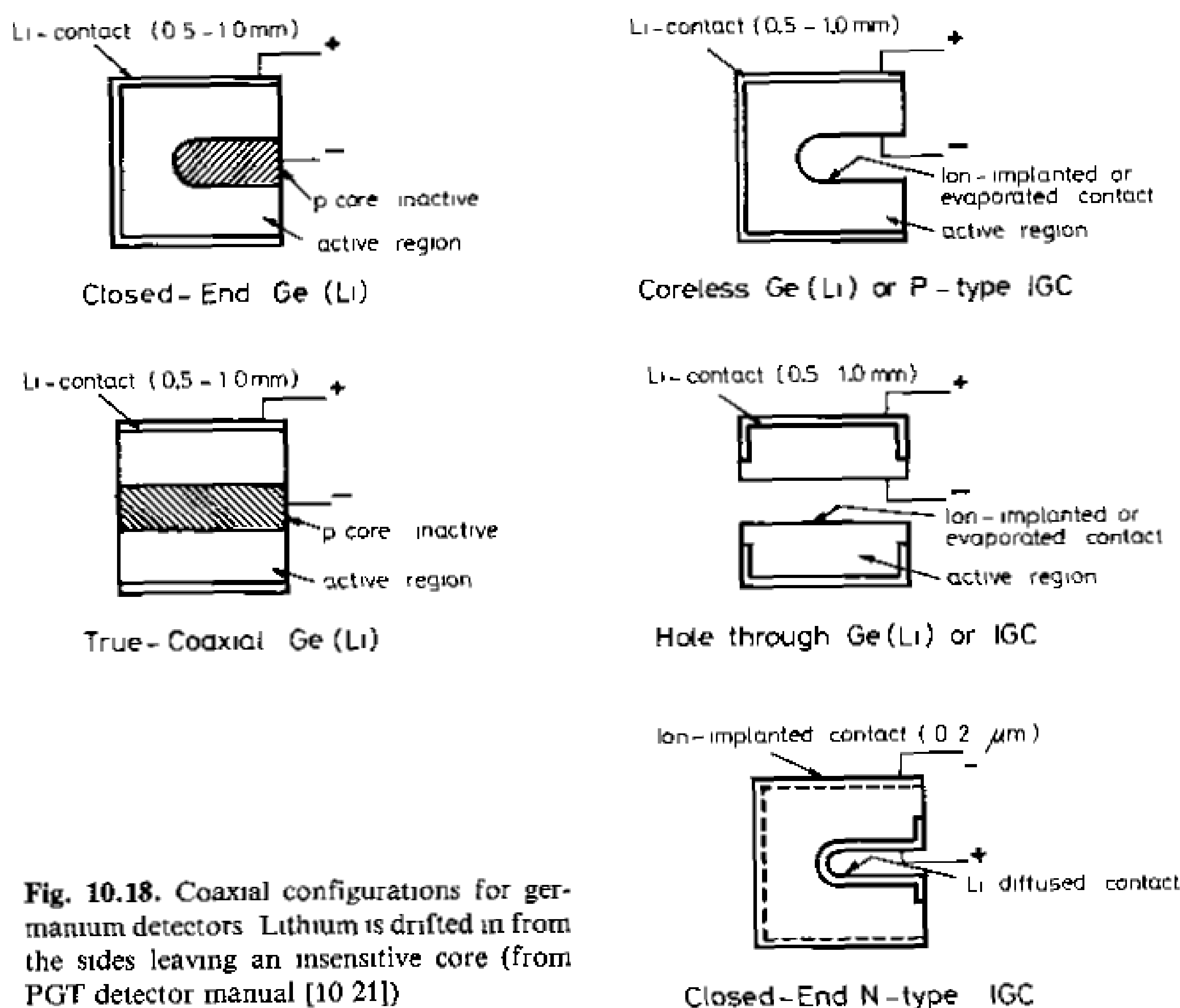

Fig. 10.18. Coaxial configurations for germanium detectors Lithium is drifted in from the sides leaving an insensitive core (from PGT detector manual [10 21])

This requires mounting the crystal in a mechanically rigid cryostat with an accompanying dewar for liquid nitrogen. This, of course, puts severe constraints on the experimental geometries which can be used with germanium detectors. Nevertheless, detectors with various cryostat positions and dewars are available commercially.

The sensitivity of coaxial Ge(Li) detectors is generally limited by the thickness of the dead layer formed on the face of the crystal by lithium drifting and the cryostat window which absorb low-energy photons. Typical limits are on the order of 30 keV. For planar detectors, the window contact can be made from a thin layer of gold which results in a lower limit on the order of a few keV.

A more complete discussion of the operating characteristics of Ge(Li) detectors is given in the book by *Knoll* [10.12].

10.7.2 Intrinsic Germanium

In more recent years, advances in semiconductor growth technology have allowed the fabrication of very high purity germanium with impurity concentrations of less than 10^{10} atoms/cm^3. Detectors of this type have the advantage of not having to be kept at low temperatures at all times Cooling is only necessary when a high voltage is applied.

Intrinsic germanium (also called HPGe for *High Purity Germanium*) detectors are constructed and operated in the same way as Ge(Li) detectors and are now gradually replacing the latter. One advantage with intrinsic detectors is the possibility of using n-type semiconductor rather than the p-type required for the lithium-drifting process. A very thin window can then be formed by ion-implantation to extend the sensitivity of

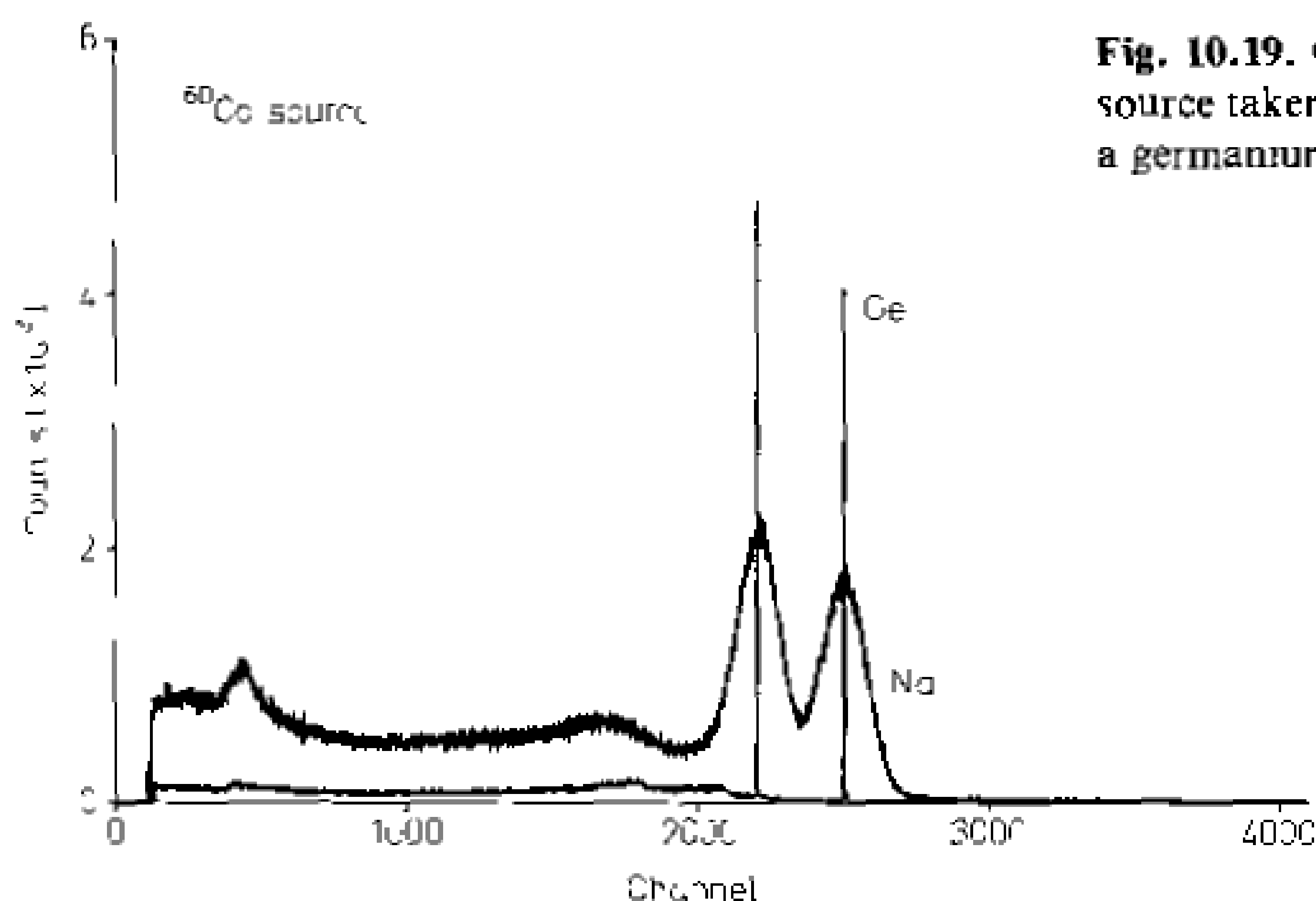

Fig. 10.19. Comparison of spectra from a ^{60}Co source taken with a NaI detector (*top curve*) and a germanium detector

the coaxial detector to below 10 keV. These detectors are also somewhat more resistant to radiation damage.

10.7.3 Gamma Spectroscopy with Germanium Detectors

The principal application of germanium detectors is gamma ray spectroscopy. At present, germanium detectors offer the highest resolution available for gamma-rays energies from a few keV up to a 10 MeV. This is illustrated in Fig. 10.19 which compares the spectrum from ^{60}Co taken with a NaI detector to the same spectrum as measured by an intrinsic Ge detector. The difference is quite dramatic: at 1.33 MeV the Ge resolution is about 0.15% while for NaI this value is ~8%! In addition, the peak to Compton ratio is much greater due to the higher photoelectric cross section of germanium.

For precision spectrum measurements, the energy resolution and signal to noise ratio are the most important parameters. It is important therefore to shield the detector with lead so as to minimize background. The signal-to-noise ratio can also be increased with the use of an optical feedback preamplifier. Attention should also be paid to the count rates. These should not be too high so as to avoid pile-up effects which can distort the spectrum.

In order to measure the absolute intensities, a calibration of the absolute detection efficiency is necessary. This must be performed with calibration sources which span the energy region of interest. Gamma sources whose outputs are calibrated to within 1 or 2% can be obtained commercially. In most cases, it is the *full peak efficiency*, i.e., the efficiency for photoelectric conversion, which is desired. This is given by the total count rate in the photopeak for each gamma-ray divided by the total output of the source. The Compton scattered part is ignored.

Attention must be paid to the source-detector geometry. The calibration must be performed at the source-to-detector distance to be used and this distance must be reproducible. It is a good idea to construct a rigid source holder which mounts onto the detector so as to insure this reproducibility. Another factor is the size of the radioactive sources to be measured. If these are distributed sources, this must also be taken into account in the calibration. Most commercial calibration sources can be considered as point-like and it may be possible to simulate the distributed source by displacing the calibration source off-axis and measuring the efficiency for several points. The total efficiency can then be estimated by integrating over these measured points.

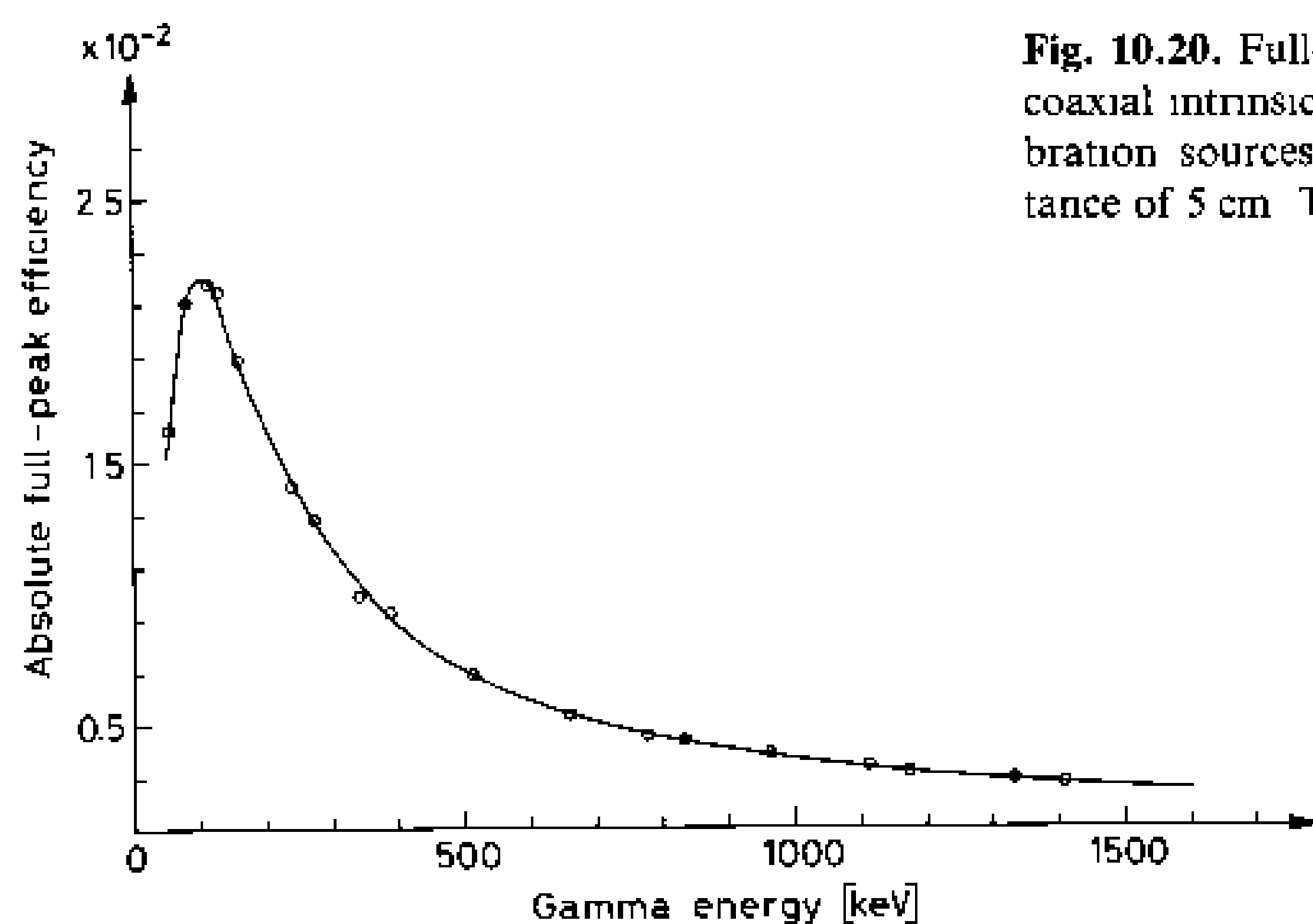

Fig. 10.20. Full-peak efficiency curve measured for a coaxial intrinsic germanium detector Point-like calibration sources were used at a source-detector distance of 5 cm The curve is a piecewise polynomial fit

As with spectrum measurements, it is important to keep the count rate at reasonable levels. If possible the calibration should be performed at these rates. At high rates, accidental coincidences between two gamma-rays from the same source can reduce the number of counts in their true gamma-ray peaks by pile-up. The two gamma rays are thus registered at an energy corresponding to their sum rather their individual energies. This *summing-effect* is particularly important for sources emitting many cascade photons. If the decay scheme and emission angles between all the gamma rays are known, the effect can, in principle, be calculated. However, for most sources this is generally not possible.

Figure 10.20 shows a measured full-peak efficiency curve for a coaxial intrinsic germanium detector at a source-to-detector distance of 5 cm. The points are fitted piecewise by polynomial functions. A number of empirical forms have also been proposed to describe the form of this curve [10.22].

A final factor to consider is the effect of dead time which can also lead to distortion as well as losses. This is discussed in Sect. 5.5.

10.8 Other Semiconductor Materials

Because germanium must be cooled during operation, a good deal of effort is being put into finding new high-Z semiconductor materials which can be operated at room temperature. Many compounds have been investigated, however, only two show some promise as of this moment. The first is cadmium telluride (CdTe) which is commercially available and the second mercuric iodide (HgI_2) which is still under development.

Cadmium telluride was the first material (other than silicon) to have been developed as a room temperature detector. It has an energy gap of 1.45 eV and atomic numbers of 48 and 52. This, of course, makes it highly efficient for gamma ray detection. Mercuric iodide has an even higher Z (80 and 53) and an energy gap of 2.14 eV. The average energy for electron-hole creation is somewhat higher than Si and Ge being on the order of 4.4 eV.

While these detectors present many favorable properties for gamma detection, they are still fraught with many problems. Mercuric iodide, in particular, is plagued by in-

complete charge collection caused by hole trapping and polarization effects leading to space charge build-up which limit its efficiency and resolution. CdTe is on somewhat firmer ground and is now sold commercially. In both cases, however, it is still difficult to fabricate large volume detectors from these materials because of nonuniformities. The low yield of good crystals also makes them very expensive.

Research and development are still continuing in these domains and it is hoped that a better understanding of the physics of these materials will allow more reliable detectors to be constructed. For a review of the current status of these detectors, the reader is referred to [10.2, 26].

10.9 Operation of Semiconductor Detectors

10.9.1 Bias Voltage

The bias voltage, as we saw in (10.23) and (10.24), determines the thickness of the depletion layer and also the capacitance of the detector. Higher voltages thus reduce the noise by increasing the depletion thickness; however, a greater risk of breakdown is also incurred. For commercial detectors, the optimum bias values are supplied by the manufacturer and should not be surpassed. Typical values for SSB's, for example, range from 50 – 300 V while for germanium detectors these voltages can be as high as 4000 – 4500 V.

When voltage is applied, this should be done slowly, raising the voltage a few tens of volts at a time and allowing the detector to "*settle*" for a few seconds after each step. A good procedure is to observe the noise signal on the oscilloscope as the voltage is raised. Immediately after each increase in voltage, the signal may disappear from the oscilloscope display but should reappear after a second or two. If there are any sudden, intermittent increases in noise, this is a sign of incipient breakdown and one should proceed slowly allowing more settling time. If there is a sudden, very large increase in noise, breakdown has occurred and the voltage should be removed immediately to prevent irreversible damage. After the desired voltage has been reached, it is a good idea to allow the detector to stabilize for a few hours, especially if it has not been used for a long period. In some cases, the noise level will also diminish further.

Particular care should be taken with very thin detectors as small increases in voltage correspond to large increases in the electric field intensity. A 10 Volt increase on a 20 μm detector, for example, corresponds to an electric field increase of 5000 V/cm!

In the case where the operating voltage is unknown, the bias may be determined by observing the noise level on an oscilloscope while *slowly* raising the applied voltage. The noise amplitude should diminish to some minimum and then slowly rise again. Setting the voltage at the minimum point then should normally provide the best results. Needless to say, care should be taken not to apply too much voltage

10.9.2 Signal Amplification

Because of the small signals obtained from semiconductor detectors, care must be taken to use low-noise electronics for signal processing In particular, a preamplification is necessary before any further treatment can be made. Because the capacitance of semiconductors change with temperature, this is performed by a *charge-sensitive* preampli-

fier which, after the detector itself, is the second most important part of a semiconductor detector system. This type of preamplifier is preferred because of its insensitivity to changes in capacitance at its input as described in Sect. 14.1 To ensure stability, it is necessary for the preamplifier capacitance to be much larger than all other sources of capacitance at the input, i.e., the detector, cables, etc. Since typical detector capacitances are on the order of ten's of picofarads, preamplifier dynamic capacitances are generally on the order of a few 10's of nanofarads. With very thin SSB's, however, the detector capacitance can approach 1 or 2 nF, in which case, higher preamplifier capacitance would be required for optimum performance.

The noise of the preamplifier is particularly important as it affects the ultimate resolution of the detector. Since the signal from the detector appears as electric charge, electronics noise is usually quantified by giving its *equivalent noise charge* (ENC). If V_{rms} is the average voltage noise level appearing at the output, then

$$\mathrm{ENC} = e\frac{V_{rms}}{w}C \ , \tag{10.40}$$

where C is total input capacitance of the detector and preamplifier and w the average energy required to create an electron-hole pair. The noise may also be expressed in terms of an equivalent energy corresponding to the ENC. This is usually given as a peak width [i.e., the full width at half maximum (FWHM)] using the relation

$$\frac{\mathrm{FWHM}}{2.35\,w} = \mathrm{ENC} \ . \tag{10.41}$$

From (10.40), it is clear that minimizing noise requires minimizing the input capacitance to the preamplifier. For this reason, the preamplifier is generally mounted as close as possible to the detector in order to reduce capacitance from cables, etc. Coupling to the detector can be performed either directly (dc coupling) or through an additional capacitor (ac coupling) [10.27]. These are diagrammed in Fig. 10.21. For high resolution operation at low temperatures, such as with germanium gamma-ray detectors, a direct coupling is made for the minimum in input capacitance. A direct coupling also allows monitoring of the leakage current which is an advantage. An inconvenience, however, is that neither electrode of the detector is at ground potential which implies some additional work in designing the detector mounts to ensure a good insulation. Typical noise values range from less than 1.5 keV at 0 input capacitance to 18 keV at 1000 pF [10.28].

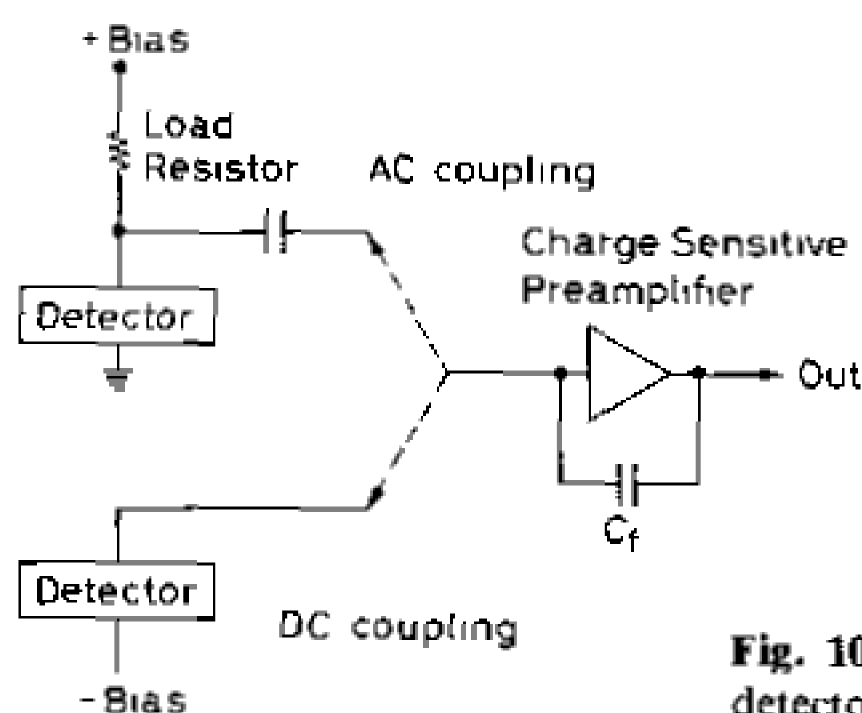

Fig. 10.21. AC and DC coupling of preamplifiers to semiconductor detectors (after *Goulding* and *Landis* [10.27])

For charged particle spectroscopy with room temperature detectors, the ac coupling method is generally quite adequate. In this configuration, one electrode is grounded which facilitates mounting, however, the additional load capacitor contributes to the noise. If the particles are of sufficiently high energy, however, the effect is usually minimal.

For fast timing applications, such as time-of-flight measurements, in which a timing signal, as well as an energy signal from the detector are desired, some additional considerations must be made. If the collection time of the detector is greater than the rise-time of the preamplifier, then both energy and timing signals may be derived from the same charge-sensitive preamplifier. Very often, however, the detector is a thin, high capacitance dE/dx detector in which the collection times are much shorter. In such cases, a hybrid system involving charge-sensitive and voltage sensitive or current sensitive preamplifiers might be necessary. These and other timing problems are reviewed by *Spieler* [10.29]

10.9.3 Temperature Effects

As we have seen, temperature has an important effect on the conductivity of the detector. Germanium detectors must *always* be operated at low temperatures otherwise the high leakage current will cause irreversible damage to the crystal.

For silicon detectors, increasing temperature will also result in higher leakage currents and greater noise. For each 10 °C rise in temperature, there is roughly a three-fold increase in the leakage current [10.28]. The maximum temperature limit for silicon is generally between 45° to 50 °C at which point breakdown occurs.

Decreasing the temperature with silicon detectors, of course, greatly reduces noise. However, the expansion coefficients of the mounting should first be considered before cooling. In particular, the bonding epoxy could crack if it is not made to withstand low temperatures. Another point to be aware of, is that the band gap for silicon increases by about 0.1 eV (see Table 10.1) when going from room temperature to liquid nitrogen temperatures For the same gain on the associated electronics, there will therefore be a slight shift between spectra recorded at these two temperatures.

10.9.4 Radiation Damage

As we have mentioned, semiconductor detectors are relatively sensitive to radiation damage. Incident particles colliding with lattice atoms cause point defects by "knocking" them out of their normal positions. These structural defects then give rise to discrete trapping levels in the forbidden band gap which reduce the number of charge carriers in the semiconductor. There also appears to be changes in the resistivity of the base material as well. A review of the radiation damage problem can be found in [10.30]

The main effects of radiation damage on detector performance are an increased leakage current and a degradation of energy resolution. In more heavily damaged detectors, double peaks in spectra have also been reported. If the damage is not too great, however, an increase in the bias voltage can compensate resolution loss to some extent by decreasing the collection time.

For a given fluence[2] of radiation, the increase in leakage current can be estimated through the relation

[2] The fluence is defined as the total accumulated number of particles incident per unit area It is thus the integral of the particle flux over time

Table 10.3. Damage constants in silicon for various radiations (from [10.25, 26])

Particle type	K [cm^2/s]	
	n-type	p-type
Electrons		
3 MeV	$2-10\times10^{-8}$	3×10^{-9}
Muons		
GeV	1.4×10^{-7}	
Neutrons		
Fission	0.5×10^{-5}	2.5×10^{-6}
1 MeV	1×10^{-5}	2.5×10^{-6}
14 MeV	2×10^{-6}	0.7×10^{-6}
Protons		
2 MeV	2×10^{-8}	
20 MeV	$2-10\times10^{-5}$	1.3×10^{-5}
207 MeV	5×10^{-6}	2×10^{-6}
590 MeV	1.2×10^{-6}	0.9×10^{-6}
3 GeV	10^{-6}	
24 GeV	3.8×10^{-8}	

$$J = q n_i d K \frac{\phi}{2} \tag{10.42}$$

where ϕ is the radiation fluence, n_i the intrinsic carrier concentration from (10.1), d the depletion depth, and K the damage constant which depends on the radiation type and its energy. Table 10.3 summarizes some measured damage constants for various radiations at different energies. By choosing the maximum tolerable leakage current, the maximum allowable fluence for a given type and energy of incident radiation can be calculated by inverting (10.42).

10.9.5 Plasma Effects

For very heavily ionizing particles, i.e., heavy ions, fission fragments, etc., the high density of electron-hole pairs created in semiconductors leads to space-charge phenomena which affect the rise time and pulse height of the resulting signal. In effect, the high ionizing power of these particles produces a dense cloud of space charge along the particle trajectory which locally nullifies the external applied electric field. The charge in the cloud, therefore, is not immediately swept up. Gradually, of course, diffusion dissipates the cloud and the charge is collected after a characteristic delay time.

This delay affects the signal in a number of ways:

1) The risetime of the pulse is much slower since the effective collecting field is much lower. This change in risetime is known as the *plasma time*.
2) During the delay, electrons and holes in the cloud have time to recombine so that total collected charge is less than what is created. This leads to what is called *pulse height defect*.

The main consequence of pulse height defect is that the detector calibration is different for different particle types. In general, the energy-pulse-height relation can be given by a formula [10.31, 32] of the type

$$E(X, M) = (a + a_1 M)X + b + b_1 M \ , \qquad (10.43)$$

where E is the energy of the ion, M, its mass and X the pulse height. The coefficients a, a_1, b and b_1 are experimentally determined by measuring the spectrum of fission fragments from a standard source such as ^{252}Cf. A new formula based on more recent measurements has also been proposed by *Ogihara* et al. [10.33].